Diagnostic impact of the cyst fluid telomerase activity measurement using droplet digital PCR for predicting the histologic grade of cystic neoplasms of the pancreas

博士論文

Diagnostic impact of the cyst fluid telomerase activity measurement using droplet digital PCR for predicting the histologic grade of cystic neoplasms of the pancreas

（デジタル PCR を用いた膵嚢胞液中のテロメラーゼ活性測定は

嚢胞性膵腫瘍の良悪性の鑑別診断に有用である）

東北大学大学院医学系研究科医科学専攻

外科病態学講座　消化器外科学分野

畠　達夫

Abbreviations

AUC	:	Area under the curve
CEA	:	Carcinoembryonic antigen
CT	:	Computed tomography
dd-TRAP	:	Droplet digital-telomeric repeat amplification protocol
ddPCR	:	Droplet digital polymerase chain reaction
EUS	:	Endoscopic ultrasonography
EUS-FNA	:	Endoscopic ultrasonography-guided fine needle aspiration
HGD	:	High-grade dysplasia
IC	:	Internal control
ICG	:	International consensus guideline
IGD	:	Intermediate-grade dysplasia
IPMN	:	Intraductal papillary mucinous neoplasm
LGD	:	Low-grade dysplasia
LOB	:	Limit of blank
LOD	:	Limit of detection
MCN	:	Mucinous cystic neoplasm

MPD : Main pancreatic duct

MRI : Magnetic resonance imaging

PanNET : Pancreatic neuroendocrine tumor

PCR : Polymerase chain reaction

ROC : Receiver operating characteristic

SCN : Serous cyst neoplasm

SD : Standard deviation

SPN : Solid pseudopapillary neoplasm

TRAP : Telomeric repeat amplification protocol

Abstract

Pancreatic cystic tumors have a wide range of malignant potential and it is therefore crucial to predict the presence of malignancy with reliable diagnostic accuracy in order to decide surgical indication. Although preoperative imaging and clinical findings, combined with cyst fluid molecular markers, have increased the diagnostic performance, diagnostic accuracy remains less than satisfactory. To improve the diagnostic performance of telomerase activity for predicting the malignancy of pancreatic cystic tumors, I quantified the telomerase activity using a combination of droplet digital PCR platform and a telomerase repeat amplification protocol (dd-TRAP). This resulted in the higher detection sensitivity and a wider quantifiable range compared to the conventional method. Using this technique, telomerase activity was measured in surgically-aspirated cyst fluid samples from 184 patients who underwent pancreatic resection for a cystic lesion: 118 with intraductal papillary mucinous neoplasm, 45 with serous cystadenoma, 13 with other cystic neoplasms, and 8 with pseudocyst. I found telomerase activity was reduced in samples that had been previously thawed. Among unthawed samples, I revealed that cyst fluids with invasive cancer and high-grade dysplasia showed the higher telomerase activity (median [interquartile range], 1299 [830.2–11980] copies/μL of cyst fluid) than those without

counterparts (23.1 [3.3–344.8] copies/μL, $P < 0.001$). Cyst fluid telomerase activity >730 copies/μL had a sensitivity of 83.3% and a specificity of 90.0% for predicting the invasive cancer/high-grade dysplasia. Among cysts classified preoperatively as having "worrisome features", cyst fluid telomerase activity had high diagnostic performance (sensitivity, 92.3%; specificity, 86.5%; accuracy, 88.0%). In multivariate analysis, telomerase activity was an independent predictive factor associated with malignancy. Absolute quantification of telomerase activity using the dd-TRAP assay could be a powerful diagnostic tool for predicting the malignancy with in a pancreatic cysts.

Background

Due to the improvement and widespread use of high-resolution multimodality imaging, management of pancreatic cystic tumors are increasingly being acknowledged during the past two decades[1)]. Pancreatic cystic tumors encompass a wide spectrum of malignant potential from benign to borderline to malignant[1, 2)]. Serous cystic neoplasms (SCN)s are usually benign and have low potential of malignancy in nearly all the cases, and when asymptomatic, they can be managed by surveillance based on computed tomography (CT)/magnetic resonance imaging (MRI) imagining[3)]. Mucinous cystic neoplasms (MCN)s should be resected without any surveillance because of their malignant potential[4)]. Solid pseudopapillary neoplasms (SPN)s are also recommended to be resected at the time of diagnosis[5)]. Intraductal papillary mucinous neoplasms (IPMN)s have a wide spectrum of pathological malignancy ranging from low-grade dysplasia (LGD) to invasive cancer. Only high-grade dysplasia (HGD) and invasive cancer should be resected and LGD and intermediate grade dysplasia (IGD) should be managed by surveillance[4)].

Currently, differential diagnosis and surgical indication of pancreatic cystic tumors is based on the clinical symptoms and imaging findings. For predicting the possible presence of malignancy and surgical indication, the International Consensus Guidelines

(ICG) 2012 has stratified the specific clinical and imaging findings based on CT/MRI into "worrisome features" and "high-risk stigmata"[4]. In accordance with the diagnostic algorithm, surgical intervention is recommended for cases with "high-risk stigmata" while only the cases with "worrisome features" should undergo the endoscopic ultrasonography (EUS) analysis for further evaluation. In addition to the imaging findings, EUS-guided cyst fluid cytology and biomarker analysis have been utilized for the differential diagnosis of pancreatic cystic tumors[6]. Both cytology and carcinoembryonic antigen (CEA) analysis using EUS with fine-needle aspiration (EUS-FNA) are highly specific (95.0% and 83.0%, respectively)[7]; however, these analyses show false-negative results (33.0% for cytology and 7.7% for CEA) mainly because of sampling errors[8, 9]. Therefore, novel biomarkers with higher diagnostic accuracy are urgently needed.

Telomerase is a key enzyme in the immortalization of malignant neoplasms and its elevated activity has been detected in various human cancers including pancreatic cancer[10, 11]. Previous reports investigating pancreatic juice samples have demonstrated the diagnostic utility of telomerase activity for differentiating the pancreatic cancers from benign pancreatic tumors with high sensitivity and specificity[12-14]. Furthermore, recent meta-analysis revealed that the telomerase activity measurement in pancreatic juice sample

showed the higher diagnostic performance than the four major genetic marker (*KRAS*, *CDKN2A/p16*, *TP53*, and *SMAD4/DPC4*) for the differential diagnosis of pancreatic cancer[15]. As for the pancreatic cystic tumors, Hashimoto et al. showed the higher telomerase activities in invasive cancer tissue arising from IPMN and HGD than in either IGD or those in LGD IPMN[16]. Furthermore, telomerase activity in solid components and thickened walls of pancreatic cystic lesions obtained by imaging-guided biopsies was higher in malignant tumors than in benign tumors and pancreatic pseudocysts[17]. However, telomerase activity measurements in these studies were based on the tissue samples, and no previous reports have evaluated telomerase activity using bulk aspirated cyst fluid samples.

The most common method used to measure the telomerase activity is the telomerase repeat amplification protocol (TRAP) assay, developed in 1994[18]. Briefly, this assay involves three steps. First, endogenous telomerase in cell or tissue extracts extends the synthesized oligonucleotide with telomeric repeats. Next, these extended products are specifically amplified by PCR using upstream and downstream primers. Finally, electrophoresis and subsequent densitometries for PCR products are conducted to measure telomerase activity as a ratio of the internal control[18]. Even though the improvement of this method with some modification, this method need laborious polyacrylamide gel

electrophoresis and subsequent densitometric analysis of 6-bp telomeric ladder[19-21]. Moreover, because of the non-quantitative and relative activity measurement compared with that of the reference sample, at least ~ 2-fold difference of telomerase activity can be detectable on the basis of this conventional gel-based TRAP assay (gel-TRAP assay)[20, 22]. Taken together, further improvements are required to apply high-throughput measurement without multiple experimental steps and reference samples in each reaction.

Droplet digital PCR (ddPCR), a recently developed technique, involves emulsification and PCR amplification inside the thousands of nanolitter scale droplets, each droplet containing one or no molecules of target DNA[23-25]. Simple, precise, and reproducible absolute quantification of the number of target DNA can be conducted by counting the number of positive droplets at the endpoint PCR thermocycling without the need of a standard curved or the consideration of the amplification rate. Recently, Ludlow et al. applied ddPCR with EvaGreen double strand DNA binding dye to the second step of the TRAP assay and compared the performance in terms of diagnostic resolution, quantifiable range, and reproducibility between the conventional gel-TRAP assay and the newly developed ddPCR-based TRAP (dd-TRAP) assay in various types of culture cells[26]. They revealed that dd-TRAP assay exhibits greater precision, better reproducibility and a

wider detectable ranges compared to the gel-TRAP assay[26]. These results suggest that the dd-TRAP strategy can be applied for high-throughput analyses of clinical samples.

Aim

In the present study, to investigate the applicability and practicality of the dd-TRAP assay for clinical samples and increase the diagnostic performance for predicting the presence of malignancy within a pancreatic cyst using quantitative telomerase activity measurement, I applied dd-TRAP assay to surgically aspirated cyst fluid samples.

Materials and Methods

Ethics

All elements of this study were approved by the institutional review board of Johns Hopkins Medical Institutions and written informed consent was obtained from all enrolled patients.

Patients and specimens

Patients with pancreatic cystic tumor who had undergone surgical resection at the Department of Surgery, Johns Hopkins Hospital between 2008 to October 2015 were included in this study. Patients' characteristics, clinical symptoms, preoperative imaging findings such as CT, MRI, and EUS with cyst fluid cytology and CEA values were obtained from hospital records. I classified the imaging findings on the basis of CT/MRI into "high-risk stigmata", "worrisome features", and "low risk" following the ICG 2012 algorism[4]. Details of clinical and imaging findings of each risk group are shown in Table 1. A cut-off value of CEA in cyst fluid was set to 192 ng/mL according to the previous report[27]. The pathology of the surgically resected tumor was reviewed by pancreatic pathologists. The decision to surgical resection for each case is based on multiple factors

including not only the potential risks of malignancy within a cyst but also the clinical symptoms caused by an enlarged cyst and the age, performance status, and co-morbidity of patient. All of cyst fluid samples were harvested from resected pancreatic cystic tumor. Cyst fluid samples were aspirated from the resected cyst in the surgical pathology suite immediately after the surgical resection using a fine needle sterile syringe and stored immediately at 4 °C and then transferred on ice to the laboratory generally within two hours, where it was aliquoted and stored at – 80 °C. All cyst fluid samples utilized in this study had been prospectively collected in institutional fluid and tissue bio-bank in a standardized fashion. All experiments and data analysis were conducted in a blinded fashion, without any prior knowledge of pathological diagnosis.

Cell culture

Human pancreatic cancer cell lines MiA PaCa-2, BxPC-3, Hs 766T, PANC-1, AsPC-1, CFPAC-1, Capan-1, Capan-2, and SU.86.86 were obtained from the American Type Culture Collection (Rockville, MD, USA) and A38-5 was obtained from the investigator who created the line [Dr. James Eshleman (Johns Hopkins University, Baltimore, MD, USA)]. An immortal human pancreatic duct epithelial cell line, HPDE, was

kindly provided by Dr Ming-Sound Tsao (University of Toronto, Ontario, Canada). All cell lines, except for HPDE, were cultured in Dulbecco's modified Eagle's medium (Life Technologies, Inc., Gaithersburg, MD, USA) supplemented with 10% fetal bovine serum (Mediatech, Inc., Manassas, VA, USA) and 1% antibiotics (Pen/Strep; Life Technologies) and incubated at 37 °C in a humidified atmosphere of 5% CO_2 in air. HPDE cells were cultured in keratinocyte serum free medium supplemented by bovine pituitary extract and epidermal growth factor (Life technologies).

Protein extraction

Following harvesting, I determined the original volume of cyst fluid applied to the analyses in accordance with the visual inspection in predicting the sufficient yield of protein, at least 1 μg. The average volume of cyst fluid used to isolate protein was 400 μL (range, 40–1,000 μL). Cells were pelleted down by centrifugation at 5,000 rpm for 5 min. Supernatant was aspirated and discarded. According to the previous study, precipitated cells were lysed in NP-40 buffer (10 mM Tris-HCl, pH 8.0, 1 mM $MgCl_2$, 1 mM EDTA, 1% (vol/vol) NP-40, 0.25 mM sodium deoxycholate, 10% (vol/vol) glycerol, 150mM NaCl, 5mM β-mercaptoethanol, 0.1mM AEBSF (4-[2-aminoethyl] benzenesulfonyl fluoride

hydrochloride)) for a 30 min on ice[26]. The lysate was then centrifuged at 15,000 rpm for 20 min at 4 °C and the supernatant collected as the cell extract. Protein concentration was measured by BCA method using Pierce BCA Protein Assay Kit − Reducing Agent Compatible (Thermo Fisher scientific, Waltham, MA, USA) and stored at – 80 °C until ready for further analyses. I repeated the protein extraction procedures by adding the equal volume of NP-40 lysis buffer into the remaining pellet until there was no longer any lysed protein detectable. For cyst fluid samples, 1 to 5 μg of protein extract (depending on the yield of extracted protein from the original cyst fluid) was applied to further analysis.

gel-TRAP assay

The first step for TRAP assay is the extension reaction. In brief, endogenous telomerase in cell extracts can catalyze addition of varying numbers of TTAGGG hexameric repeats onto the 3' end of a telomeric TS primer[20, 26]. One μg of protein extracts from cell line pellets were applied and incubated with 50 μL of extension reaction mixture containing 1 × TRAP reaction buffer (10 × concentration: 200 nM Tris-HCl, pH 8.3, 15nM $MgCl_2$), 0.4 mg/mL bovine serum albumin, TS primer (200 nM; 5'-AATCCGTCGAGCAGAGTT-3'), dNTP (2.5 mM each, Thermo Fisher scientific) at

25 °C for 60 min.

The second step is to amplify the extension reaction products by PCR. The total volume of the gel-TRAP PCR reaction mixture was 25 μL and contained 1 × ThermoPol® Reaction Buffer (New England Biolabs, Ipswich, MA, USA), 12.5 ng of TS primer, 0.125 μL of TRAP primer mix [ACX primer (5'-GCGCGGCTTACCCTTACCCCC TAACC-3'), NT primer (5'ATCGCTTCTCGGCCTTTT-3'), and TSNT primer (5'-AATCCGTCGAGCAGAGTTAAAAGGCCGAGAAGCGAT-3')] as previously described[21], 1 U of *Taq* DNA polymerase (New England Biolabs), 50 μM of each dNTP and 2 μL of extraction reaction mixture (i.e. × 0.04 dilution of cell extracts in 50 μL of extension reaction mixture). The PCR reaction was then started at 95°C for 5 min, followed by a 30 cycles of 3 steps amplification (95 °C for 30 sec, 54 °C for 30 sec, and 72 °C for 30 sec). Following PCR, reaction mixtures were analyzed by electrophoresis in 0.5 × Tris-borate-EDTA buffer on 12% polyacrylamide non-denaturing gels and visualized with ethidium bromide staining. The images were then processed and quantified by densitometry using ImageJ® software (National Institutes of Health, Bethesda, MD, USA). Telomerase activity at the ratio of the intensity of 6-bp ladder to that of internal control (IC) was calculated based on the following formula: ((intensity of sample's 6-bp ladder) –

(background intensity between the sample lanes))/intensity of sample's IC band[21]. The experimental workflow of the gel-TRAP assay is shown in Figure 1.

Droplet digital TRAP assay

For ddPCR, each 20 μL reaction setup contained 1 × ddPCR EvaGreen Supermix (Bio-Rad, Hercules, CA, USA), 50 nM of TS and ACX primer, 2 μL of extension reaction mixture (the same as for the gel-TRAP assay described above). The 20 μL droplet ddPCR reaction mixture was then loaded into the DG8 disposable droplet generator cartridge (Bio-Rad). A volume of 70 μL of droplet generation oil was loaded into the oil well for each sample. The cartridge was placed into the Droplet Generator QX200 (Bio-Rad). This draws both the PCR reagents and oil through a flow-focusing nozzle where around 20,000 individual droplets ~1 nL in size are formed, suspended in an emulsion. Following droplet generation, the water-in-oil droplet emulsions were transferred to a 96-well polypropylene PCR plate (twin.tec PCR plate; Eppendorf, Hauppauge, NY, USA). The plate was heat-sealed with foil using a PX1 PCR Plate Sealer (Bio-Rad) and placed in a Veriti Thermal Cycler (Applied Biosystems). Thermal-cycling conditions were 95°C for 5 minutes (1 cycle), was followed by 37 cycles of 95 °C for 30 sec, 54 °C for 30 sec, 72 °C

for 30 sec. A dye-stabilization step was also included at the end of thermal cycling protocol (4 °C for 5 min then, 95 °C for 5 min, and finally at 12 °C indefinite hold). The temperature ramp rate was set to 2.5 °C/sec, and the lid was heated to 105 °C, according to the manufacture's recommendations. After the thermal cycling, droplet reading was performed on a QX200 ddPCR Droplet Reader (Bio-Rad), which automatically reads the droplets from each well of the plate. Analysis was done using QuantaSoft 1.7.4 Analysis software (Bio-Rad) and the target concentration (copies/μL; PCR scale) was then computed using Poisson statistics. Figure 1 shows the study workflow of the dd-TRAP assay and the conventional gel-TRAP assay. In the present study, to best reflect the nature of original cyst fluid, absolute quantification of telomerase products per microliter of original cyst fluid was calculated using the following formula: telomerase product (copies)/PCR volume (20 μL) × PCR volume (20 μL)/extracts applied to PCR (μg) × total yield of protein extracts (μg)/ original cyst fluid volume (μL).

Optimization of dd-TRAP assay for absolute quantification

I attempt to estimate the limit of detection (LOD) in accordance with the previous reports[28, 29]. To determine the limit of blank (LOB) of telomerase activity using dd-TRAP

assay, I first performed the 60 replicates of ddPCR with 5 technical replicates using the 12 different extraction reaction mixtures containing only NP-40 lysis buffer as blank samples. Sample processing of mixtures was performed on several different days considering the consistency across the study periods. Pooled data were assumed to follow a Gaussian distribution. When $\alpha = 0.05$, the LOB is estimated by the 95th percentile of the distribution of the blank samples.

$$LOB = M_b + 1.645 \times SD_b$$

where M_b stands for the mean of blank sample data and SD_b for the combined standard deviation (SD) of the blank sample data. I next performed ddPCR with 20 replicates in each 2 extract with different low concentration of 0.0008 μg and 0.00032 μg, respectively. When $\beta = 0.05$, the LOD is estimated by the 95th percentile of the distribution of the low concentration samples. LOD estimate can be expressed in a following formula as

$$LOD = LOB + c_\beta \times SD_s$$

where SD_s stand for the combined SD of the low concentration sample data and c_β, the multiplicative factor that is associated with the target acceptable error risk of false negative, is calculated as follows:

$$c\beta = \frac{1.645}{1 - \frac{1}{4(Ns - \kappa)}}$$

where *Ns* means the total number of replicates and κ means the number of samples.

According to the estimated LOD, the actual copies above LOD considered to be quantifiable. In the present study, I used a half value between LOB and LOD for the actual values between them. For the actual value below LOB, I used as “zero”.

Statistics

The non-parametric Wilcoxon signed-rank test was used to compare continuous variables. The chi-square test was used to compare categorical variables. Correlations between two different variables were assessed by scatter-plot and R^2 value. The diagnostic accuracy of telomerase activity in predicting the presence of malignancy was assessed by receiver operating characteristics (ROC) curve analysis. The cut-off value was defined as the result with the highest sensitivity and specificity that lay closest to the left upper corner of the curve. A multivariate analysis using the logistic regression model was performed including the variables with significant by univariate analysis. Statistical analysis was performed using the JMP Pro 11.0.0 statistical software (SAS Institute Inc., Cary, NC, USA) and GraphPad Prism V6.0 (GraphPad Software, San Diego, CA, USA). *P*-value of less than 0.05 was considered to indicate statistical significance.

Results

dd-TRAP assay using pancreatic cancer cells lines

First, I detected telomerase activity by the dd-TRAP assay using pancreatic cancer cell lines. Figure 2A shows a representative result of the dd-TRAP assay using 2 of the 50 μL the extension reaction mixtures (i.e. 0.04 of 1 μg cell extracts) derived from the MiA PaCa-2 cell line with negative controls. As negative controls, cell extracts were treated with RNase A (37 °C for 20 min) or with heat (95 °C for 5 min) and then applied to PCR reaction. Both the RNase A pre-treatment and heat inactivation drastically decreased the number of signals. Considering the evidences that the PCR products amplified by the TRAP assay contains multiple size of amplicons known as 6-bp ladder, I set a manual threshold above the negative cluster in 1-D plot in each well. Figure 2B shows the actual accepted total droplets in each lane (16,000–18,000 droplets), indicating successful droplet generation in the dd-TRAP method, which contained diluted cell extracts. Figure 2C shows the concentration of telomerase products corresponding to Figure 2A after the computational analysis using Poisson statistics. I extracted the DNA from the droplets after the PCR reaction and analyzed the size of amplicons by electrophoresis on a polyacrylamide gel and it was detectable that 6p-ladder as telomerase product. The image

was similar to conventional gel-TRAP assay (Figure 2D).

Linearity and limit of detection of the dd-TRAP compared to the gel-TRAP assay

In order to investigate the diagnostic utility of the dd-TRAP assay in terms of the wider detectable range and higher detection sensitivity than the gel-TRAP assay, I compared the telomerase activity between the dd-TRAP and the gel-TRAP assay using the serial dilution of MiA PaCa-2 cell extracts. Figure 3A and 3B shows the result of electrophoresis and subsequent densitometry of the gel-TRAP assay, where I could not detect the 6-bp ladder in lanes containing 4 ng or less of the applied cell extracts. Furthermore, relative intensities were saturated in lanes containing 500 ng or more. Therefore, I estimated that the dynamic range of measurement for relative intensity was from 8 ng to 500 ng of cell extract. On the contrary, the dd-TRAP assay detected telomerase activity in lanes containing 0.32 ng to 2,500 ng of cell extract (Figure 3C and 3D). To ensure the robust quantification within a low concentration range, I attempted to determine the LOD. Figure 3E shows the LOD value for telomerase activity based on dd-TRAP is 0.468 (telomerase products/μL; PCR scale). Based on the LOD, the dynamic quantifiable range of the dd-TRAP technique is from 2,500 ng of applied cell extracts

(1,734 copies/μL) to 0.8 ng (0.59 copies/μL) with high linearity (R^2 = 0.99657), indicating a wider range and higher linearity compared to the gel-TRAP assay (Figure 3F).

Comparison of dd-TRAP to gel-TRAP assay using pancreatic cancer cell lines

It is known that the pancreatic cancer cells demonstrate the various degrees of telomerase activity, partially depending on the cell growth and aggressiveness[30]. I measured telomerase activities in 10 pancreatic cancer cell lines and one immortalized pancreatic ductal epithelial cell line (HPDE). Figure 4A and 4B shows the actual telomerase activities using the gel-TRAP and dd-TRAP assays, respectively. Notably, previous results reported by the HPDE established group revealed that the HPDE cell line had considerable telomerase activity[31], which is consistent with the present results (Figure 4B and 4C). To ensure the consistency of telomerase activity measurement between the dd-TRAP and gel-TRAP assays, I compared the relative telomerase activity, using levels of MIA PaCa-2 cells as a reference. Figure 4D shows a positive correlation (R^2 = 0.91498) between the two different assays, but the dd-TRAP assay demonstrates a wider range of detection than the gel-TRAP. Taken together, dd-TRAP is more sensitive and linear and has a wider range of detection than gel-TRAP.

Patient population

A total of 202 cyst fluid samples were initially collected, but I excluded 18 cases for the reasons shown in Figure 5. Therefore, the cohort of the present study consisted of 184 patients (Figure 5). The characteristics of all included patients are shown in Table 2. There were 118 patients with IPMN, 12 with MCN, 45 with SCN, 8 with a pseudocyst, and 1 with a pancreatic neuroendocrine tumor (PanNET). To assess the influence of protein integrity on overall results, I then stratified samples into subgroups according to the freeze/thaw repeats and the length of sample storage.

Absolute quantification of telomerase activity in pancreatic cystic fluid

As shown in Table 2, cyst fluid samples were heterogeneous across the specimens in terms of the volume, appearance, and color, and it was hypothesized that this heterogeneity might affect the efficiency of protein lysis processing and the subsequent results of the analysis. Actually, the median and range of the original volume of cyst fluid used for the analysis was 400 (40–1,000) μL, and the median concentration of cell extract after the first lysis processing was 1.23 μg/μL. To verify the validity of the telomerase

activity measurement per original cyst fluid samples, I investigated and analyzed the feasibility of the dd-TRAP assay using pancreatic cyst fluid samples regarding the following points. First, Figure 6A shows the total yield of protein from MiA PaCa-2 cells, lysed into NP-40 buffer at different concentrations. Irrespective of lysed concentration, there were no remaining proteins in the pellet of MiA PaCa-2 cells after three repeats of lysis processing. As for the 184 clinical cyst fluid samples, the repeat number for lysis processing varied across the samples ranging from one to seven repeats, to accomplish complete protein extraction (Figure 6B). Overall, complete protein extraction could be obtained within three repeats for 87% of all samples. I next measured the cell-free telomerase activity in the supernatant of cyst fluid and ensured that it was negligible compared with that in whole cell extracts derived from precipitates (Figure 7). I then investigated and analyzed the linear correlation between the loading cell extracts and detectable telomerase products per PCR scale. Figure 8 shows the linear correlation between the amount of cell extracts applied to the analysis and telomerase products. Finally, to investigate the inter-day reproducibility, I repeated the experiments on four different days. The day before day 1, I divided the sample into four aliquots for each experimental day. On each day, I performed the protein extraction from aliquots and the subsequent

analytic procedures independently. Figure 9 shows the reproducibility of similar results across replicates (coefficient of variation ~ 20%). These results suggest that the telomerase product copies per microliter of original cyst fluid as a unit of absolute quantification are acceptable.

Stratification of cyst fluid samples according to the protein integrity

Since the dd-TRAP assay measures enzymatic activity and therefore needs samples of optimal quality, I determined if cyst telomerase activity was affected by length of storage at –80 °C or by the effects of freeze/thawing (some samples from each diagnostic group had previously undergone one or more freeze/thaws) (Table 3). I found evidence that prior freeze/thawing, but not length of storage, was associated with reduced telomerase activity (Figure 10). Therefore, to the best reflect of robust measurement of telomerase activity, I performed the further analysis focusing on the unthawed samples from 84 patients. Table 4 shows the characteristics of these 84 patients whose samples had not undergone prior freeze/thawing.

Diagnostic performance of the telomerase activity in pancreatic cyst fluid

Among these 84 patients, higher levels of telomerase activity were detected in the cyst fluid of IPMN cases with HGD compared to IPMN cases with IGD, cases with SCN, or cases with a pseudocyst ($P < 0.001$, Figure 11A). I also compared cyst fluid telomerase activity in the most relevant diagnostic groups: cases with IPMN and HGD +/- an associated invasive cancer vs. those with IPMN and either IGD or LGD ($P < 0.001$), and vs. SCN ($P < 0.022$), respectively (Figure 11B). There was no significant difference in telomerase activity between cyst fluids from IPMNs with an associated invasive cancer and those from IPMNs with HGD only ($P = 0.280$, Figure 11A). The median value and interquartile range of telomerase activity levels in each group are shown in Figure 11C. Among all 84 cases, the telomerase activity level (cut-off value: 730 copies/μL of cyst fluid) with the best overall accuracy for distinguishing cyst fluids with invasive cancer/HGD vs. those from IGD/LGD had an area under the curve (AUC) of 0.890; for the 58 IPMN cases the AUC was 0.853 (Figure 11D and 11E, respectively). In this series, telomerase activity had higher diagnostic sensitivity (83.3%) than other clinical parameters for distinguishing IPMNs with invasive cancer or HGD from IPMNs with lower grade dysplasia (Table 5).

I also evaluated the diagnostic accuracy of telomerase activity in the cases whose

cyst fluid samples had undergone multiple (2 or 3) rounds of thawing and re-freezing and found that the differences in telomerase activity between the IPMN invasive cancer/HGD group versus the IPMN IGD/LGD group were still statistically significant and had similar diagnostic accuracy (Figure 12). Additionally, the diagnostic performance of cyst fluid telomerase activity for whole study population, analyzed without regard for sample thawing, was very similar to the subset of cyst fluid samples without multiple freeze/thaws. Telomerase activity was significantly higher in the IPMN invasive cancer /HGD cases compared to IPMN cases with IGD, cases with LGD, and cases with SCN, and the diagnostic accuracy was only slightly less (AUC 0.832 for IPMN cancer /HGD vs. IPMN IGD/LGD) (Figure 13). The diagnostic accuracy of telomerase activity was not increased significantly by combining this measurement with other clinical parameters (Table 6).

SCN samples showed the low telomerase activity irrespective of freeze/thaw repeats, and ranged from 0–294.4 copies/μL of cyst fluid. It is well known that the blood cells such as lymphocytes have low telomerase activity and there is a possibility that a bloody sample might demonstrate higher telomerase activity. Since some SCN cyst fluid samples are bloody, and since there is modest levels of telomerase activity in inflammatory cells, I also investigated if bloody cyst fluid samples from SCN cases had higher telomerase

measurements. I did find that SCN cyst fluid samples with a bloody appearance had slightly higher levels of telomerase activity than those with a serosanguinous or clear appearance (Figure 14).

Predictive factors of malignancy for pancreatic cystic tumors

Among 84 samples without prior freeze/thawing, I performed univariate analysis and found five significant factors predicting the malignancy: mucinous cystic fluid appearance ($P < 0.0001$), a main pancreatic duct (MPD) size larger than 5 mm ($P < 0.0001$), the presence of MPD communication ($P = 0.0004$), presence of mural nodule ($P = 0.0093$), and telomerase activity above 730 copies/μL of original cyst fluid ($P < 0.0001$) (Table 7). Furthermore, only telomerase activity was an independent malignant predictor in the subsequent multivariate analysis (odds ratio: 41.488, 95% confidence interval: 4.897–992.730, $P = 0.0002$, Table 7).

Subgroup analysis stratified according to the preoperative risk group

To evaluate the diagnostic accuracy of cyst fluid telomerase activity measurements in relation to the pre-operative evaluation of patients, I classified the study

population by their clinical features into those with “high-risk stigmata”,“worrisome features”, and “low risk” as defined by the ICG 2012[4]. Among the 84 cases, 11 (57.9%) of 19 cases with “high-risk stigmata” and 13 (26.0%) of 50 cases with “worrisome features” had invasive cancer or HGD (Figure 15). Among the 50 cases with “worrisome features”, telomerase measurements had a diagnostic sensitivity of 92.3% for distinguishing those with invasive cancer or HGD from those with lower grades of dysplasia (Cut off: 730 copies/μL of original cyst fluid) and an AUC of 0.927 (Table 8). Among the 58 IPMN cases, 31 had worrisome features, and telomerase activity in this group had a similarly high diagnostic performance (AUC of 0.876) for distinguishing those with invasive cancer or HGD from those with lower grades of dysplasia (Cut off: 730 copies/μL).

Telomerase activity in endoscopically aspirated cyst fluid

To evaluate the utility of telomerase activity measurement for preoperative diagnosis, I compared the telomerase activities in endoscopically aspirated cyst fluid samples with those in matched surgically aspirated samples. Although statistical analysis could not be performed because of the small sample size, telomerase activity in both endoscopically and surgically aspirated cyst fluid from the case of IPMN with HGD was

the highest among the three matched three cases (Table 9). Similar values for telomerase activity were measured between the endoscopically and surgically aspirated cyst fluid samples in cases No. 1 and 2. However, telomerase activity was much higher in the surgically aspirated cyst fluid than that in the endoscopically aspirated samples in case No. 3 of IPMN with HGD (Table 9).

Discussion

In the present study, I conducted absolute quantification of telomerase activity using the dd-TRAP assay, which showed powerful diagnostic performance for the presence of malignancy within a pancreatic cyst. The present study is the first report with regard to two notable findings. First, combining the TRAP assay with the ddPCR method, namely the dd-TRAP assay, is applicable and practical for clinical samples. Second, telomerase activity measurement in pancreatic cyst fluid samples is useful for predicting malignancy of pancreatic cystic tumors.

Ludlow AT, et al. first developed the dd-TRAP assay and demonstrated the linearity and reproducibility of quantification of telomerase activity from a variety of cell types such as tissue culture cells and primary adult human cells[26]. Although the gel-TRAP assay was well established and widely used, and still remains to be sufficient for the qualitative or semi-quantitative measurement of telomerase activity, the utility of this method for clinical samples is considered not be feasible. Using the conventional gel-TRAP assay, telomerase activity was measured as relative values for internal controls and/or reference samples, meaning that there is a lack of precise quantification. Furthermore, polyacrylamide gel electrophoresis and subsequent gel staining or autoradiography steps

are required to visualize the 6-bp ladder and to quantify telomerase activity, which takes a lot of time. Recently, a real-time quantitative PCR based TRAP assay has been reported by several groups[21, 32-35]. Even though this method allows for a more quantitative analysis of telomerase activity rather than the gel-TRAP method, data analysis regarding setting of an amplification threshold and quantifiable range of Ct value remains debatable[34, 35]. In contrast, the dd-TRAP assay allows for the precise quantification of telomerase activity and needs neither standard samples, internal controls, nor electrophoresis. Therefore, the dd-TRAP assay can be a potential diagnostic tool for high-throughput screening of telomerase activity using clinical samples.

One of the most important analytical processes for the ddPCR platform was to set the exact position of the threshold value for distinguishing the positive from negative droplets. Despite the simplicity of the principle that positive droplets derived from amplified PCR products with intercalating dye have higher fluorescence amplitude than the negative droplets without PCR products, there is no well-established method for how to set an exact threshold line especially in samples with intermediate signals between positive and negative clusters[36]. Apart from the usual PCR assay, the TRAP assay has unique characteristics since it contains multiple amplicon sizes, depending on telomerase activity.

Actually, greater numbers of EvaGreen molecules are capable of binding to larger amplicons, meaning that higher fluorescence amplitude is observed in longer PCR products than in shorter ones[37]. In the present study, as shown by Ludlow AT et al., the dd-TRAP assay produced a considerable number of intermediate signals where no clear discrimination was observed between positive and negative droplets. Negative control samples with RNase A treatment and heat inactivation abolished the almost all the positive and intermediate signals. Furthermore, for an unknown reason, a shift in the baseline as negative droplet cluster in 1-D plot across samples was observed. Taken together, intermediate signals between the positive and negative cluster of droplets were considered as "positive". For the present analysis, I manually set the threshold line just above the negative clusters by visual interpretation, which was shown to be a reliable method for analysis.

Another important note about the data interpretation and analysis is the rate of false positive. Since the development of the TRAP assay, the efforts to reduce primer dimer formation have been attempted, because the TRAP assay is usually based on the amplification of telomeric repeats using fixed primer pairs[18]. Previous reports developed the ACX primer, having a 6 bp anchor at the 5'-end and a new permutation of the telomeric

sequence, resulted in the significant reduction of primer dimer formation[20]. However, as shown in previous reports, the present study revealed that very minor background signals were observed in non-template controls[26], partially because of high detection sensitivity of the ddPCR platform. To assess the robustness of detection and quantification, I determined the LOB and LOD prior to clinical sample analysis. Actually, LOB was estimated to be 0.153 copies/μL of PCR scale and these very minor background signals might be derived from the multiple factors of non-specific amplicon, primer-dimer formation, and incidental contamination of exogenous protein.

For the clinical specimen, to best reflect the nature of original cyst fluid, absolute quantification of telomerase products per microliter of original cyst fluid was calculated and applied to further analysis following the formula described in Materials and Methods. Actually, the actual amount of cell extracts applied to the extension reaction mixture varied across the specimens ranging from 1.0–5.0 μg, because part of the cyst fluid samples with lower cellularity contained very low amounts of protein. Moreover, telomerase activity derived from non-cancerous cells such as lymphocytes should be considered, especially in cases with precipitates containing a large number of blood cells. In these cases, there is a possibility that a large population of blood cells with low telomerase activity might mask

the cancer cell-derived telomerase activity. Therefore, quantification of telomerase products per microgram of cell extract might introduce bias caused by the condensation of original cyst fluid cellularity and might overestimate telomerase activity. Consequently, I believe the cellularity within original cyst fluid should be maintained in the analysis. In fact, I demonstrated complete protein extraction, no telomerase activity in cell-free protein, and linear correlation between loading amount of extracted protein and telomerase products. Taking these results together, the present study revealed that the absolute quantification of telomerase activity per microliter of original cyst fluid volume is acceptable.

According to the comments of ICG 2012, a combination of the clinical, imaging, and molecular characteristics provides the best initial preoperative diagnosis of the cyst type. If the EUS is available, consideration may be given for EUS with cytopathology, CEA, and molecular analyses. Apart from the analyses of cyst fluid cytology and CEA measurement, both of which have some limitations with low diagnostic sensitivity, the molecular and genetic biomarkers in cyst fluid are useful for predicting the biological behavior of pancreatic cystic tumors[38-41]. Recent genetic analyses revealed the specific features of gene alteration in each type of cystic tumors, including IPMN, MCN, SCN, and SPN. Springer A, et al revealed that the mutations in *GNAS* and *KRAS* were detected in

58 % and 78% of cyst fluid specimens from IPMN cases[42], similar to 66% and 81% of tissue specimens, respectively[43]. In contrast, no *GNAS* mutations were present in other cyst types. Furthermore, using the cyst fluid samples, *VHL* mutation was detected in 42% of SCN. *CTNNB1* mutation was detected in all 10 SPN cases. The authors performed the composite molecular and clinical markers and demonstrated a higher diagnostic accuracy regarding the classification of pancreatic cystic tumor types with high sensitivity (90–100%) and specificity (98–100%)[42]. However, it remains unknown whether these molecular markers combined with the clinical or imaging findings would be useful for differentiating malignant pancreatic cystic tumors from benign ones. Apart from the genetic markers in cyst fluid, Maker AV, et al demonstrated the pro-inflammatory cytokine of interleukin-1β could be a potential microenvironment marker predicting malignant IPMN with 79% sensitivity, 95% specificity, and 0.92 of AUC[44]. However, it should be noted that the authors concluded the necessity of further validation studies because of a small sample size (n = 40). The present study presents a unique diagnostic approach that relies on the measurement of telomerase enzyme activity using protein lysate derived from cyst fluid precipitates. Compared to a previous report showing the usefulness of semi-quantification of telomerase activity from tissue specimens of pancreatic cystic tumors[17], the present

study was distinguishable and notable in terms of the robust absolute quantification of telomerase activity and the usage of aspirated cyst fluid samples. Taken together, absolute quantification of cyst fluid telomerase activity measurement using dd-TRAP assay can be a potential molecular marker for predicting malignant pancreatic cystic tumors along with imaging features, cyst fluid cytology, and cyst fluid CEA measurement.

I revealed that telomerase activity could be quantifiable at a very low concentration from pancreatic cancer MIA PaCa-2 cells, 0.0008 μg (= 0.8 ng). For clinical cyst fluid specimens, at least 0.04 μg in cell extracts as ddPCR template (equivalent to 1.0 μg in extracts for extension reaction template) could be quantifiable. Considering that the median concentration of cell extracts after the first lysis was 1.23 μg/μL, further reduction of the original cyst fluid volume would be possible. Usage of large amounts of cyst fluid for analysis can be problematic, and further analysis is needed to determine the minimum and proper amount of loading samples.

In the present study, I also demonstrated that a higher diagnostic performance of telomerase activity was shown, especially in cases within the “worrisome features” subgroup. According to the ICG 2012, EUS-guided cyst fluid analysis should be considered after the initial assessment of CT/MRI only in cases with “worrisome features”. Cases with

"high-risk stigmata" should undergo surgical resection without further examination[4]. Therefore, as shown in this study, the higher diagnostic performance of telomerase activity in cases with "worrisome features" would be reasonable and preferable. One possible explanation as to why the cases with "high-risk stigmata" showed a lower diagnostic accuracy could be because about half of cases with "high-risk stigmata" were diagnosed as invasive cancer derived from IPMN. Pancreatic cysts associated with invasive cancer would be formed as a result of degeneration of the tumor due to a lack of blood supply and subsequent hypoxic condition. Otherwise, the accessory retention cysts would be formed nearby the invasive cancer due to a complete obstruction of branch pancreatic duct and accumulation of necrotic tissue of pancreatic parenchyma[45]. These cysts contain a large amount of necrotic tissue, rather than mucus, and might affect the results of analysis. Alternatively, 10–15% of human cancers, including pancreatic cancer lack detectable telomerase activity, and maintain their telomere length in a telomerase-independent manner[46].

Although the number of cases was limited, I measured the telomerase activities in endoscopically aspirated cyst fluid samples at the time of preoperative EUS-FNA and compared the surgically aspirated cyst fluid samples from the three matched cases. In one

case of IPMN with HGD, telomerase activity in the surgically aspirated sample was much higher than that in the endoscopically aspirated sample. This discrepancy may be derived from the difference in sampling methods, such as the use of different needle sizes and aspiration pressures rather than tumor progression from the preoperative EUS examination to surgical resection. Furthermore, needle size and aspiration pressure may be problematic, particularly in cases with mucinous samples. Although further improvements in harvesting devices and procedures are required to reduce sampling error, cyst fluid telomerase activity in the endoscopically aspirated cyst fluid samples is promising for providing helpful information related to surgical indication.

The present study has some limitations. I used 184 surgically aspirated cyst fluid samples and 3 endoscopically aspirated samples because almost all EUS-guided endoscopically aspirated cyst fluid samples had no histological confirmation. Although all enrolled patients in this study underwent surgical resection and therefore had defined histology, the results of analyses cannot be directly applied to patients who undergo surveillance without surgical resection. In the future, analysis of paired fluid samples collected from pre-operative EUS-guided aspiration and surgery with larger sample size is warranted to demonstrate that there is similar telomerase activity between them.

Furthermore, serially collected samples from same individual who underwent surveillance should be assessed to demonstrate the diagnostic utility for surgical indication.

Another possible limitation is the inconsistency of protein integrity in the enrolled samples. In the present study, previous thawing/re-freezing of the cyst fluid vials resulted in underestimation of telomerase activity, particularly in IPMN cases; therefore, all 184 samples were stratified according to the presence or absence of previous thawing/re-freezing. Protein integrity may also be affected by the sample collection, transportation, and dispensing steps. In the future, for sample dispensing into a large number of small vials containing protease inhibitor, a standard protocol for sample processing steps should be established to maintain protein integrity across clinical samples.

Conclusions

In conclusion, the present translational research study revealed the applicability and practicality of combining the TRAP assay with ddPCR for clinical samples. Furthermore, absolute quantification of telomerase activity measurement using dd-TRAP assay in pancreatic cyst fluid samples has potential as a predictive factor for the presence of malignancy within a cyst, and has a powerful diagnostic performance with high sensitivity and specificity compared with other clinical and imaging findings. This diagnostic accuracy was the most remarkable in cases within the "worrisome features" risk group. A further study with a large cohort, including both endoscopically and surgically collected cyst fluid samples, is warranted to confirm the validity of the present results and to elucidate dd-TRAPs usefulness for the surveillance and risk stratification of patients undergoing pancreatic screening.

Acknowledgements

Most of all, I am tremendously grateful to my advisor and mentor, Dr. Michael Goggins (Departments of Pathology, The Sol Goldman Pancreatic Cancer Research Center, Johns Hopkins Medical Institutions). His scientific curiosity inspired me to pursue my doctoral degree. He provided me the freedom and opportunity to work on various research project with world experts in pathology. He always had an open door and was willing to discuss any scientific topics. He is an excellent scientist and clinician and a trusted colleague. I thank him for his encouragement and his kindness.

I would like to thank all of present members of the Goggins lab. I especially thank Marco Dal Molin, Jun Yu, and Masaya Suenaga. Without their assistance with cell biology techniques and providing the many clinical samples, this work would not have been possible.

I would like to thank Prof. Michiaki Unno (Department of Surgery, Tohoku University Graduate School of Medicine) and Prof. Akira Horii (Department of Molecular pathology, Tohoku University Graduate School of Medicine) for providing me to a chance to go abroad for research. They also gave me wise career advise and generously offered to help in any way that would allow me to pursue my career goals.

I would like to thank all of members of Department of Surgery, Tohoku University Graduate School of Medicine. They provided various supports and assistances for my focusing on my projects.

References

1. Brugge WR: Diagnosis and management of cystic lesions of the pancreas. J Gastrointest Oncol 2015; 6: 375-388.
2. Lennon AM, Wolfgang CL, Canto MI, et al: The early detection of pancreatic cancer: what will it take to diagnose and treat curable pancreatic neoplasia? Cancer Res 2014; 74: 3381-3389.
3. Jais B, Rebours V, Malleo G, et al: Serous cystic neoplasm of the pancreas: a multinational study of 2622 patients under the auspices of the International Association of Pancreatology and European Pancreatic Club (European Study Group on Cystic Tumors of the Pancreas). Gut 2015.
4. Tanaka M, Fernandez-del Castillo C, Adsay V, et al: International consensus guidelines 2012 for the management of IPMN and MCN of the pancreas. Pancreatology 2012; 12: 183-197.
5. Law JK, Ahmed A, Singh VK, et al: A systematic review of solid-pseudopapillary neoplasms: are these rare lesions? Pancreas 2014; 43: 331-337.
6. Maker AV, Carrara S, Jamieson NB, et al: Cyst fluid biomarkers for intraductal papillary mucinous neoplasms of the pancreas: a critical review from the international expert meeting on pancreatic branch-duct-intraductal papillary mucinous neoplasms. J Am Coll Surg 2015; 220: 243-253.
7. Thornton GD, McPhail MJ, Nayagam S, et al: Endoscopic ultrasound guided fine needle aspiration for the diagnosis of pancreatic cystic neoplasms: a meta-analysis.

Pancreatology 2013; 13: 48-57.

8. Woolf KM, Liang H, Sletten ZJ, et al: False-negative rate of endoscopic ultrasound-guided fine-needle aspiration for pancreatic solid and cystic lesions with matched surgical resections as the gold standard: one institution's experience. Cancer Cytopathol 2013; 121: 449-458.

9. Cizginer S, Turner BG, Bilge AR, et al: Cyst fluid carcinoembryonic antigen is an accurate diagnostic marker of pancreatic mucinous cysts. Pancreas 2011; 40: 1024-1028.

10. Shay JW, Wright WE: Role of telomeres and telomerase in cancer. Semin Cancer Biol 2011; 21: 349-353.

11. Balcom JHt, Keck T, Warshaw AL, et al: Telomerase activity in periampullary tumors correlates with aggressive malignancy. Ann Surg 2001; 234: 344-350; discussion 350-341.

12. Zhou GX, Huang JF, Li ZS, et al: Detection of K-ras point mutation and telomerase activity during endoscopic retrograde cholangiopancreatography in diagnosis of pancreatic cancer. World J Gastroenterol 2004; 10: 1337-1340.

13. Nakashima A, Murakami Y, Uemura K, et al: Usefulness of human telomerase reverse transcriptase in pancreatic juice as a biomarker of pancreatic malignancy. Pancreas 2009; 38: 527-533.

14. Uehara H, Nakaizumi A, Iishi H, et al: In situ telomerase activity in pancreatic juice may discriminate pancreatic cancer from other pancreatic diseases. Pancreas 2008; 36: 236-240.

15. Hata T, Ishida M, Motoi F, et al: Telomerase activity in pancreatic juice

differentiates pancreatic cancer from chronic pancreatitis: A meta-analysis. Pancreatology 2016.

16. Hashimoto Y, Murakami Y, Uemura K, et al: Telomere shortening and telomerase expression during multistage carcinogenesis of intraductal papillary mucinous neoplasms of the pancreas. J Gastrointest Surg 2008; 12: 17-28; discussion 28-19.

17. Yeh TS, Cheng AJ, Chen TC, et al: Telomerase activity is a useful marker to distinguish malignant pancreatic cystic tumors from benign neoplasms and pseudocysts. J Surg Res 1999; 87: 171-177.

18. Kim NW, Piatyszek MA, Prowse KR, et al: Specific association of human telomerase activity with immortal cells and cancer. Science 1994; 266: 2011-2015.

19. Norton JC, Holt SE, Wright WE, et al: Enhanced detection of human telomerase activity. DNA Cell Biol 1998; 17: 217-219.

20. Kim NW, Wu F: Advances in quantification and characterization of telomerase activity by the telomeric repeat amplification protocol (TRAP). Nucleic Acids Res 1997; 25: 2595-2597.

21. Herbert BS, Hochreiter AE, Wright WE, et al: Nonradioactive detection of telomerase activity using the telomeric repeat amplification protocol. Nat Protoc 2006; 1: 1583-1590.

22. Krupp G, Kuhne K, Tamm S, et al: Molecular basis of artifacts in the detection of telomerase activity and a modified primer for a more robust 'TRAP' assay. Nucleic Acids Res 1997; 25: 919-921.

23. Pinheiro LB, Coleman VA, Hindson CM, et al: Evaluation of a droplet digital polymerase chain reaction format for DNA copy number quantification. Anal Chem

2012; 84: 1003-1011.

24. Hindson BJ, Ness KD, Masquelier DA, et al: High-throughput droplet digital PCR system for absolute quantitation of DNA copy number. Anal Chem 2011; 83: 8604-8610.

25. Dube S, Qin J, Ramakrishnan R: Mathematical analysis of copy number variation in a DNA sample using digital PCR on a nanofluidic device. PLoS One 2008; 3: e2876.

26. Ludlow AT, Robin JD, Sayed M, et al: Quantitative telomerase enzyme activity determination using droplet digital PCR with single cell resolution. Nucleic Acids Res 2014; 42: e104.

27. Brugge WR, Lewandrowski K, Lee-Lewandrowski E, et al: Diagnosis of pancreatic cystic neoplasms: a report of the cooperative pancreatic cyst study. Gastroenterology 2004; 126: 1330-1336.

28. Armbruster DA, Pry T: Limit of blank, limit of detection and limit of quantitation. Clin Biochem Rev 2008; 29 Suppl 1: S49-52.

29. Huang S, Wang T, Yang M: The evaluation of statistical methods for estimating the lower limit of detection. Assay Drug Dev Technol 2013; 11: 35-43.

30. Sato N, Maehara N, Mizumoto K, et al: Telomerase activity of cultured human pancreatic carcinoma cell lines correlates with their potential for migration and invasion. Cancer 2001; 91: 496-504.

31. Ouyang H, Mou L, Luk C, et al: Immortal human pancreatic duct epithelial cell lines with near normal genotype and phenotype. Am J Pathol 2000; 157: 1623-1631.

32. Jakupciak JP: Real-time telomerase activity measurements for detection of cancer.

Expert Rev Mol Diagn 2005; 5: 745-753.

33. Shim WY, Park KH, Jeung HC, et al: Quantitative detection of telomerase activity by real-time TRAP assay in the body fluids of cancer patients. Int J Mol Med 2005; 16: 857-863.

34. Hou M, Xu D, Bjorkholm M, et al: Real-time quantitative telomeric repeat amplification protocol assay for the detection of telomerase activity. Clin Chem 2001; 47: 519-524.

35. Wege H, Chui MS, Le HT, et al: SYBR Green real-time telomeric repeat amplification protocol for the rapid quantification of telomerase activity. Nucleic Acids Res 2003; 31: E3-3.

36. Trypsteen W, Vynck M, De Neve J, et al: ddpcRquant: threshold determination for single channel droplet digital PCR experiments. Anal Bioanal Chem 2015; 407: 5827-5834.

37. McDermott GP, Do D, Litterst CM, et al: Multiplexed target detection using DNA-binding dye chemistry in droplet digital PCR. Anal Chem 2013; 85: 11619-11627.

38. Hoffman RL, Gates JL, Kochman ML, et al: Analysis of cyst size and tumor markers in the management of pancreatic cysts: support for the original Sendai criteria. J Am Coll Surg 2015; 220: 1087-1095.

39. Wang J, Paris PL, Chen J, et al: Next generation sequencing of pancreatic cyst fluid microRNAs from low grade-benign and high grade-invasive lesions. Cancer Lett 2015; 356: 404-409.

40. Amato E, Molin MD, Mafficini A, et al: Targeted next-generation sequencing of

cancer genes dissects the molecular profiles of intraductal papillary neoplasms of the pancreas. J Pathol 2014; 233: 217-227.

41. Matthaei H, Wylie D, Lloyd MB, et al: miRNA biomarkers in cyst fluid augment the diagnosis and management of pancreatic cysts. Clin Cancer Res 2012; 18: 4713-4724.

42. Springer S, Wang Y, Molin MD, et al: A Combination of Molecular Markers and Clinical Features Improve the Classification of Pancreatic Cysts. Gastroenterology 2015.

43. Wu J, Matthaei H, Maitra A, et al: Recurrent GNAS mutations define an unexpected pathway for pancreatic cyst development. Sci Transl Med 2011; 3: 92ra66.

44. Maker AV, Katabi N, Qin LX, et al: Cyst fluid interleukin-1beta (IL1beta) levels predict the risk of carcinoma in intraductal papillary mucinous neoplasms of the pancreas. Clin Cancer Res 2011; 17: 1502-1508.

45. Kosmahl M, Pauser U, Anlauf M, et al: Pancreatic ductal adenocarcinomas with cystic features: neither rare nor uniform. Mod Pathol 2005; 18: 1157-1164.

46. Heaphy CM, Subhawong AP, Hong SM, et al: Prevalence of the alternative lengthening of telomeres telomere maintenance mechanism in human cancer subtypes. Am J Pathol 2011; 179: 1608-1615.

Figure and table legends

Figure 1. Experimental study workflow of the gel-TRAP and dd-TRAP assay.

Figure 2. (A) Representative result of the dd-TRAP analysis using MIA PaCa-2 pancreatic cancer cell line. **(B)** The actual accepted droplets in each sample shown in (A), showing approximately 16,000–19,000 droplets. **(C)** Target concentration (copies/μL; PCR scale) using Poisson statistics in each sample shown in (A), showing the significant lower telomerase products in negative control wells. **(D)** Gel-imaging after the electrophoresis of amplified telomerase products using the dd-TRAP assay (left side) and the gel-TRAP assay (right side). Following PCR reaction, droplets containing PCR products were treated with phenol/chloroform and extracted the amplified DNA from droplets.

HI, heat inactivation; Rn, RNase A treatment; NTC-LB, non template control lysis buffer; IC, internal control.

Figure 3. (A) Representative electrophoresis gel image of the gel-TRAP assay using the serial dilution extracts from MIA PaCa-2 cells. **(B)** Relative intensity as telomerase activity

after the densitometric analysis. **(C)** 1-D plot graphics of the dd-TRAP assay using the same serial dilution as shown in the gel-TRAP assay. **(D)** Concentration of telomerase products with Poisson 95% confidence limits. **(E)** Illustration of the relationship between LOB and LOD. For a blank sample of NTC-LB (red line), 95% of its quantification results ($\alpha = 0.05$) fall at or below LOB. For a sample with low concentration of cell extract (blue line) whose concentration equals to LOD, 95% of tis quantification results ($\beta = 0.05$) exceed the LOB. **(F)** Correlation analysis of the gel-TRAP assay and the dd-TRAP assay using serial diluted samples from MIA PaCa-2 cell extracts. R^2 means coefficient of determination.

IC, internal control; NTC-LB, non template control lysis buffer; LOB, limit of blank; LOD, limit of detection.

Figure 4. (A, B) Representative gel image and 1-D plot graphic of the gel-TRAP assay **(A)** and the dd-TRAP assay **(B)** using pancreatic cancer cell lines. **(C)** Concentration of telomerase products of the dd-TRAP assay. Error bar indicates Poisson 95% confidence limits. **(D)** Correlation analysis of gel-TRAP assay and dd-TRAP assay using 11 pancreatic caner cell lines including HPDE immortalized pancreatic ductal epithelial cell line. Relative

telomerase activity was calculated by MIA PaCa-2 cells was set 1.0 for reference. R^2 means coefficient of determination.

N, nontemplate control lysis buffer.

Figure 5. Schema of sample selection process.

Figure 6. (A) Protein concentration after the three repeats of protein extraction from the different number of MiA PaCa-2 cells. **(B)** The repeat number of protein extraction from the same precipitates in each original cyst fluid sample until lysed protein was undetectable.

Figure 7. Comparison of cell free telomerase activity in supernatant and that in precipitate from the same original cyst fluid. Serous cyst fluid samples were labeled as "S" and mucinous ones as "M".

Figure 8. Linear correlation between the loading amount of cell extract and the amplified telomerase product using dd-TRAP assay. 1-D graphics stand for the actual concentration of telomerase activity in each loading protein amount. R^2 means coefficient of

determination.

Figure 9. Coefficient of variation of telomerase activity measurements. The mean value of telomerase activity measured in three independent dd-TRAP assays measured on four different days. The horizontal bar indicates the mean value for each day. % CV means coefficient of variants calculated by the following formula: Standard deviation / Mean value × 100 (%).

CV, coefficient of variation.

Figure 10. Telomerase activity in samples sratified according to their thaw and freeze cycle and year of sample collection in each diagnostic subgroup. The longer horizontal bar represents the median value and shorter ones represents values of the 75th and 25th percentiles, respectively. $^{**}P < 0.01$, $^{***}P < 0.001$

N.S., not significant.

Figure 11. (A) Absolute quantification of telomerase activity per microliter of original cyst fluid samples among 84 samples that had not undergone any prior thawing. The longer

horizontal bar represents the median value and shorter ones represents values of the 75th and 25th percentiles, respectively. **(B)** Comparison of telomerase activity of IPMN cases classified by their surgical indication (invasive cancer and HGD vs. IGD and LGD) and SCN cases. **(C)** Telomerase activity levels per microliter of cyst fluid samples in each group. **(D, E)** ROC curve analysis for the diagnostic accuracy of telomerase activity in predicting malignancy among all 84 cases **(D)** and 58 IPMN cases **(E)**.

IQR, interquartile range; SE, standard error; CI, confidence interval. N.S., not significant.

*$P < 0.05$, ***$P < 0.001$.

Figure 12. Measurement of telomerase activity in 100 samples that had undergone multiple freeze/thaws. **(A)** Absolute quantification of telomerase activity per microliter of original cyst fluid samples. The longer horizontal bar represents the median value and shorter ones represents values of the 75th and 25th percentiles, respectively. **(B)** ROC curve analysis for the diagnostic accuracy of telomerase activity in predicting HGD/invasive cancer **(C)** Comparison of telomerase activity in IPMN cases classified by their surgical indication (invasive cancer and HGD vs. IGD and LGD) and SCN cases. **(D)** ROC curve analysis for the diagnostic accuracy of telomerase activity in predicting IPMN with HGD/invasive cancer.

SE, standard error; CI, confidence interval. N.S., not significant.

***$P < 0.001$.

Figure 13. (A) Measurement of telomerase activity using all 184 samples without accounting for sample thawing and re-freezing. The longer horizontal bar represents the median value and shorter ones represents values of the 75th and 25th percentiles, respectively. **(B)** ROC curve analysis for the diagnostic accuracy of telomerase activity in predicting HGD/invasive cancer **(C)** Comparison of telomerase activity in IPMN cases classified by the surgical indication (invasive cancer and HGD vs. IGD and LGD) and SCN cases. **(D)** ROC curve analysis for the diagnostic accuracy of telomerase activity in predicting IPMN with HGD/invasive cancer.

SE, standard error; CI, confidence interval. N.S., not significant.

***$P < 0.001$.

Figure 14. Telomerase activity of SCN cases classified into cyst fluid color. The longer horizontal bar represents the median value and shorter ones represents values of the 75th and 25th percentiles, respectively.

*$P < 0.05$.

Figure 15. Pathological diagnosis of pancreatic cystic tumors in each risk group.

Table 1. Clinical and imaging features of pancreatic cystic tumor for the aseement of preoperative risk of malignancy.

Table 2. Patient and cyst fluid characteristics for all 184 cases.

PD, pancreaticoduodenectomy; DP, distal pancreatectomy; TP, total pancreatectomy. MP, middle pancreatectomy;

*Histological grade of PanNET was diagnosed on the basis of WHO 2010 criteria.

Table 3. Length of storage and freeze and thaw repeats of surgically aspirated pancreatic cyst fluid samples.

Table 4. Patient and cyst fluid characteristics for 84 cases without prior thaw/freezing.

PD, pancreaticoduodenectomy; DP, distal pancreatectomy; TP, total pancreatectomy. MP, middle pancreatectomy;

*Histological grade of PanNET was diagnosed on the basis of WHO 2010 criteria.

Table 5. Diagnostic performance of telomerase activity comparing to the multiple imaging and clinical factors.

CI, confidence interval; PPV, positive predictive value; NPV, negative predictive value

Table 6. Diagnostic performance of combination assay for predicting invasive cancer or high-grade dysplasia among 84 cases without prior freeze/thawing

Table 7. Univariate and multivariate analyses of malignant predictive factors for pancreatic cystic tumor. Bold line indicates the statistical significance.

OR, odds ratio; CI, confidence interval.

Table 8. Diagnostic performance of telomerase activity in stratified subgroup by the risk of malignancy.

*Value of telomerase activity in pancreatic cyst fluid (copies/μL of cyst fluid).

TP, true positive; FN, false negative; FP, false positive; TN, true negative; CI, confidence interval; PPV, positive predictive value; NPV, negative predictive value.

Table 9. List of matched cases with endoscopically and surgically aspirated cyst fluid samples.

*Copies/μL of original cyst fluid

EUS, Endoscopic ultrasonography; DP, diatal pancreatectomy; PD, pancreaticoduodenectomy

Figure 1

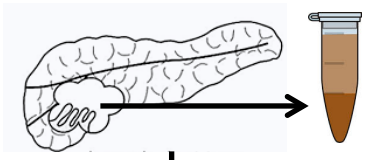

Harvest cyst fluid from the resected specimen

Protein extraction from the precipitated pellet

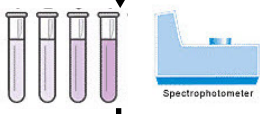

Protein Qty measurement (BCA method)

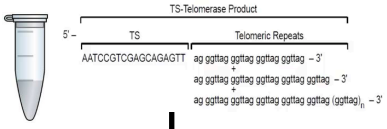

TRAP assay: Step 1
Telomerase adds telomeric repeats

gel-TRAP

dd-TRAP

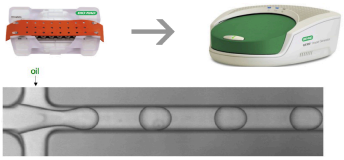

Make droplets

TRAP assay: Step 2
PCR reaction

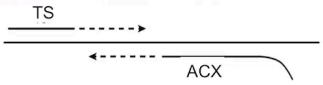

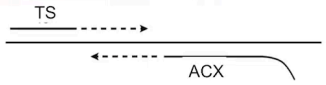

TRAP assay: Step 2
PCR reaction

Gel electrophoresis

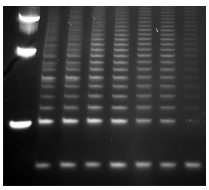

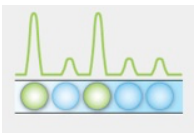

Read droplets

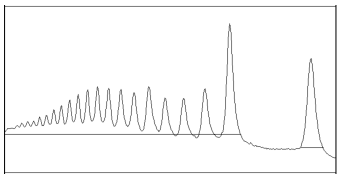

Analysis (densitometry)

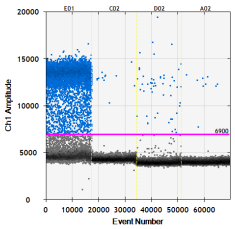

Analysis (copies/μL)

Figure 2

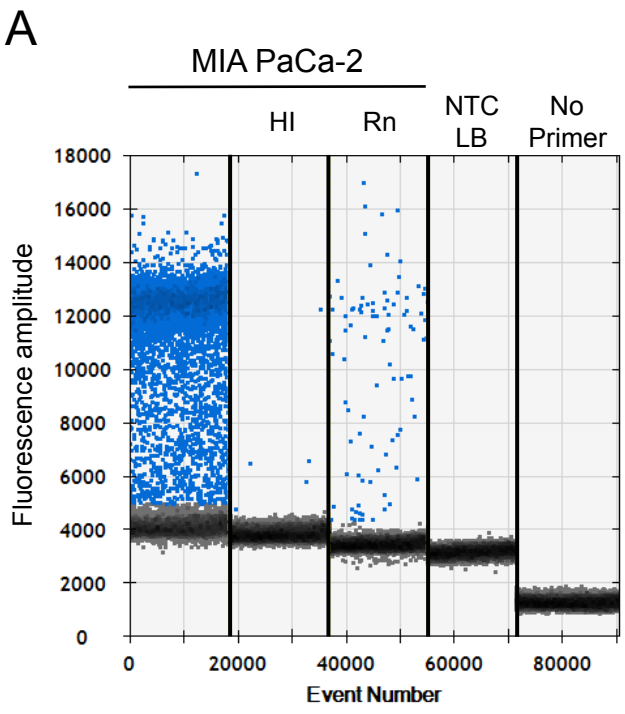
A
MIA PaCa-2
HI
Rn
NTC LB
No Primer
Fluorescence amplitude
18000
16000
14000
12000
10000
8000
6000
4000
2000
0
0
20000
40000
60000
80000
Event Number

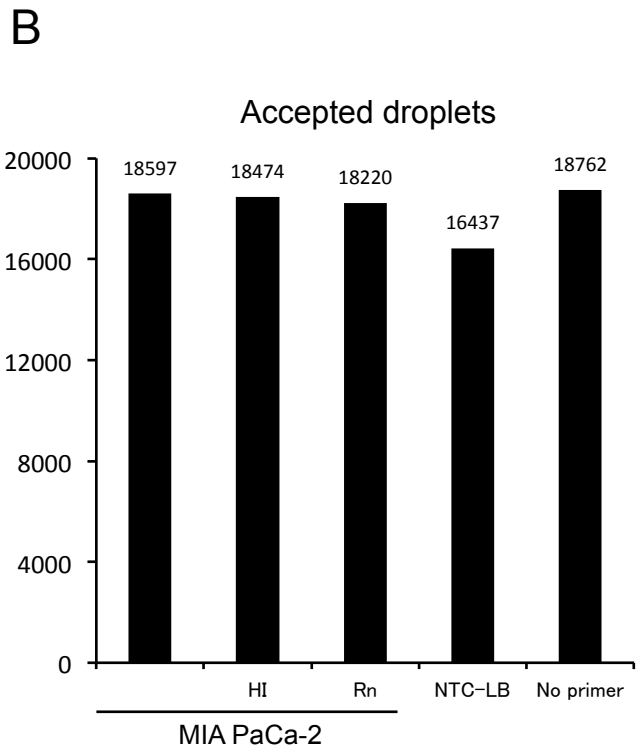
B
Accepted droplets
20000
16000
12000
8000
4000
0
18597
18474
18220
16437
18762
HI
Rn
NTC-LB
No primer
MIA PaCa-2

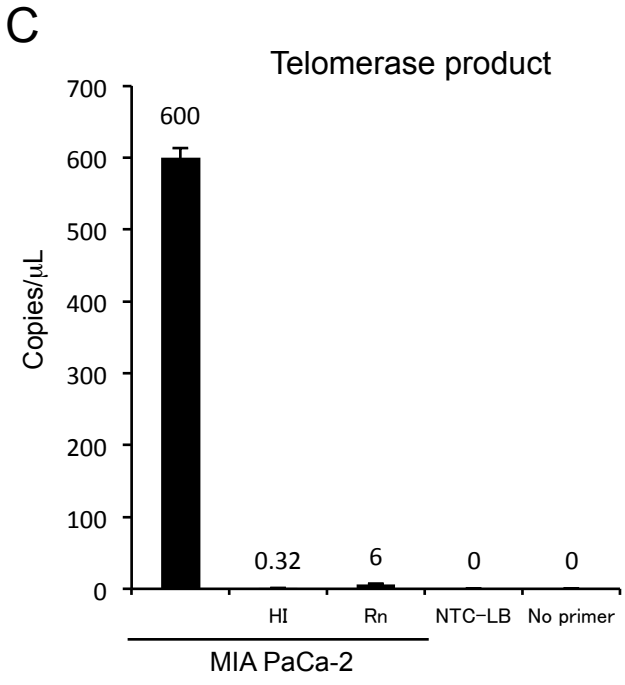
C
Telomerase product
700
600
500
400
300
200
100
0
Copies/µL
600
0.32
6
0
0
HI
Rn
NTC-LB
No primer
MIA PaCa-2

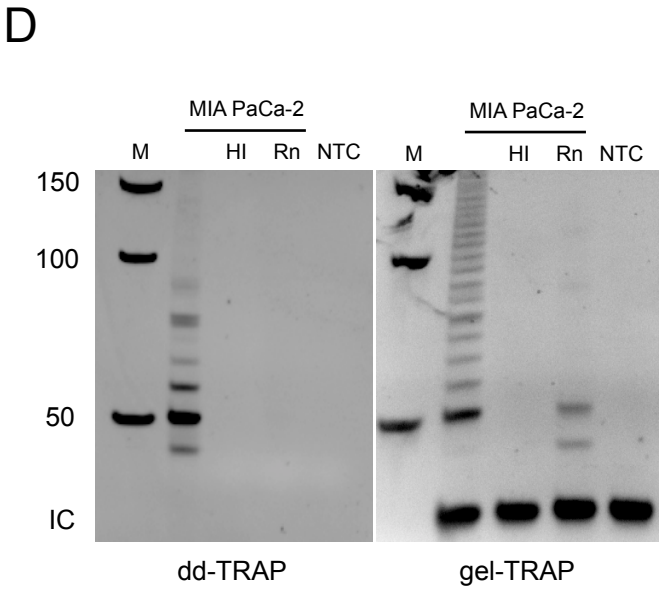
D
MIA PaCa-2
M
HI
Rn
NTC
MIA PaCa-2
M
HI
Rn
NTC
150
100
50
IC
dd-TRAP
gel-TRAP

Figure 3

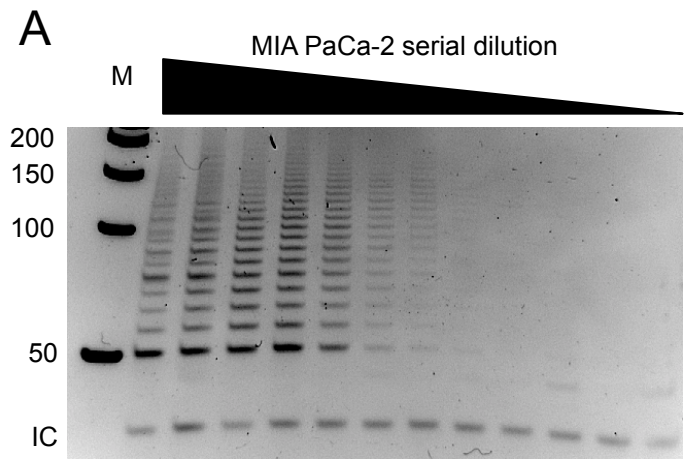
A
MIA PaCa-2 serial dilution
M
200
150
100
50
IC

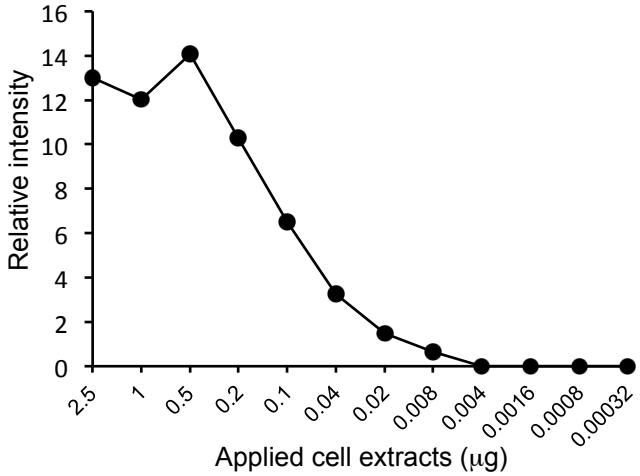
B
Relative intensity
Applied cell extracts (μg)
2.5
1
0.5
0.2
0.1
0.04
0.02
0.008
0.004
0.0016
0.0008
0.00032

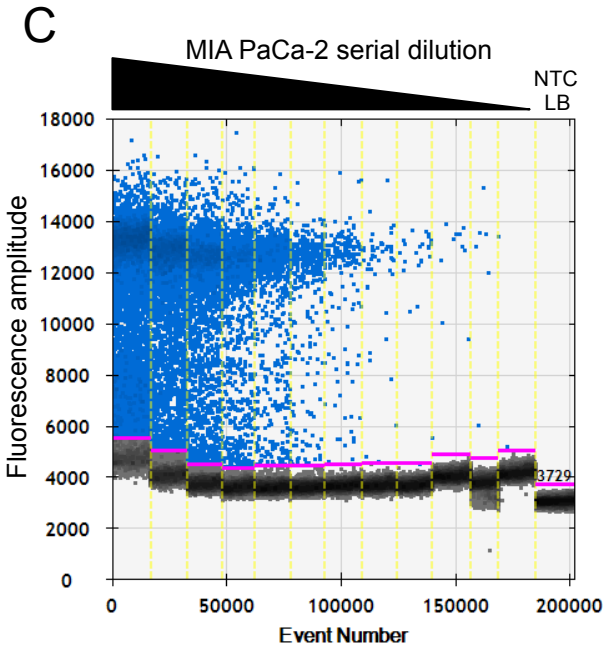
C
MIA PaCa-2 serial dilution
NTC
LB
Fluorescence amplitude
Event Number
3729

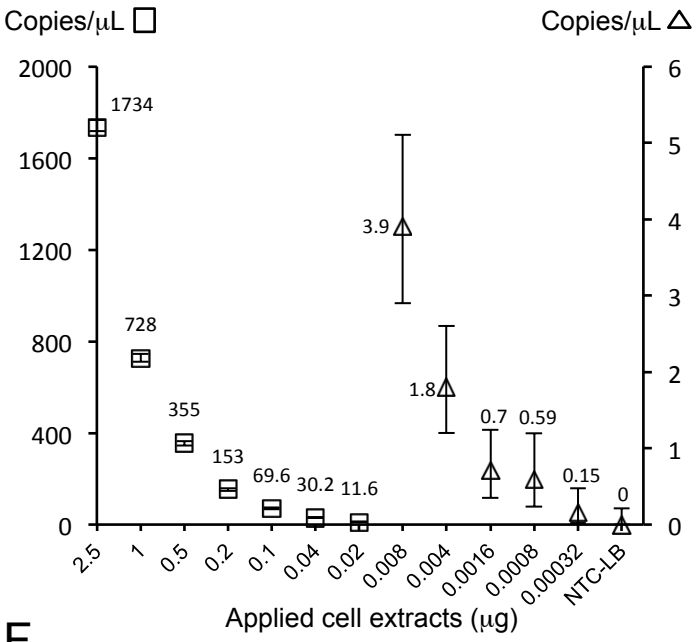
D
Copies/μL
Copies/μL
1734
728
355
153
69.6
30.2
11.6
3.9
1.8
0.7
0.59
0.15
0
Applied cell extracts (μg)
NTC-LB

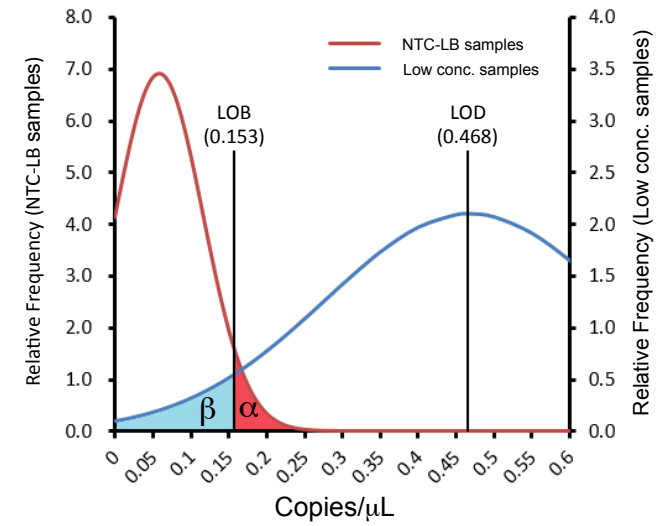
E
NTC-LB samples
Low conc. samples
LOB
(0.153)
LOD
(0.468)
β
α
Relative Frequency (NTC-LB samples)
Relative Frequency (Low conc. samples)
Copies/μL

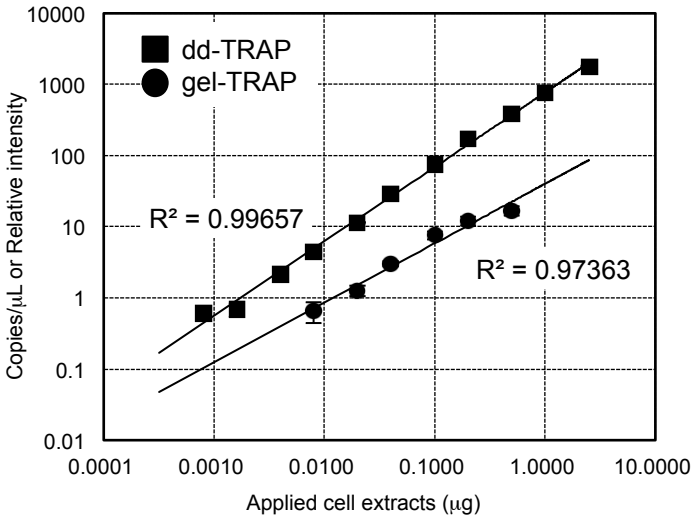
F
dd-TRAP
gel-TRAP
R² = 0.99657
R² = 0.97363
Copies/μL or Relative intensity
Applied cell extracts (μg)

Figure 4

A

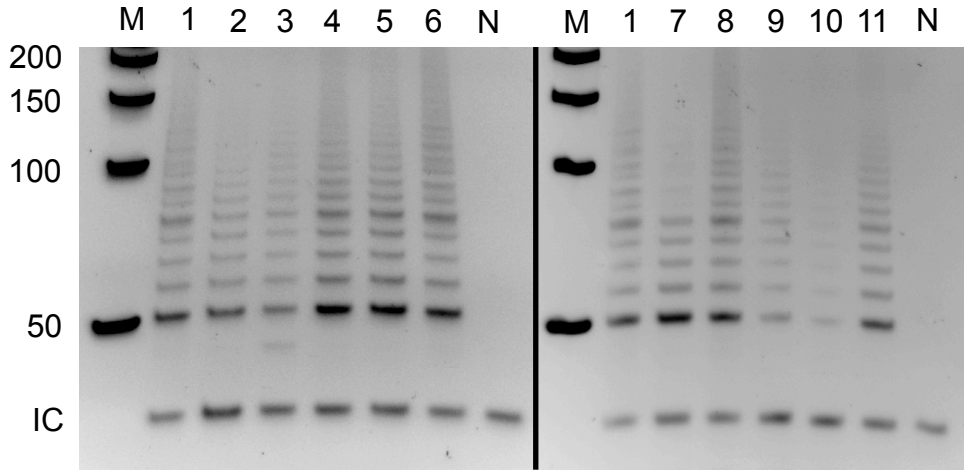

1 MIA PaCa-2
2 BxPC-3
3 Hs 766T
4 PANC-1
5 AsPC-1
6 CFPAC-1
7 Capan-1
8 Capan-2
9 A38-5
10 SU.86.86
11 HPDE
N NTC-LB

B

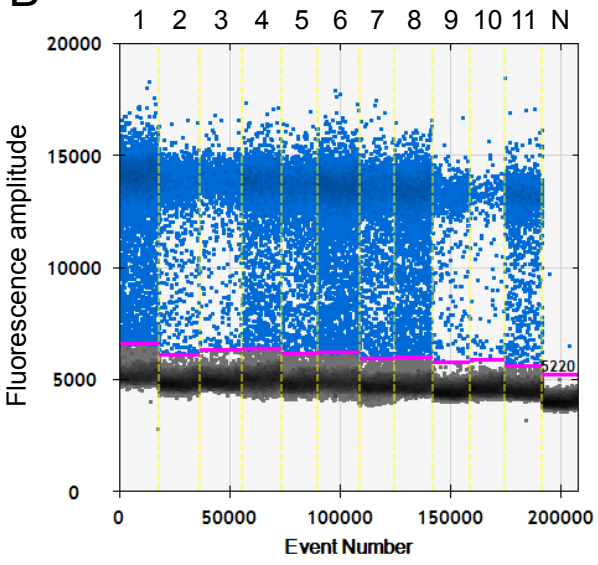

C

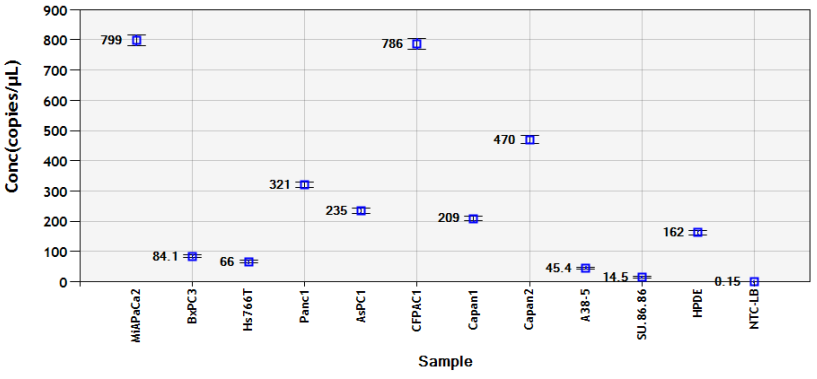

D

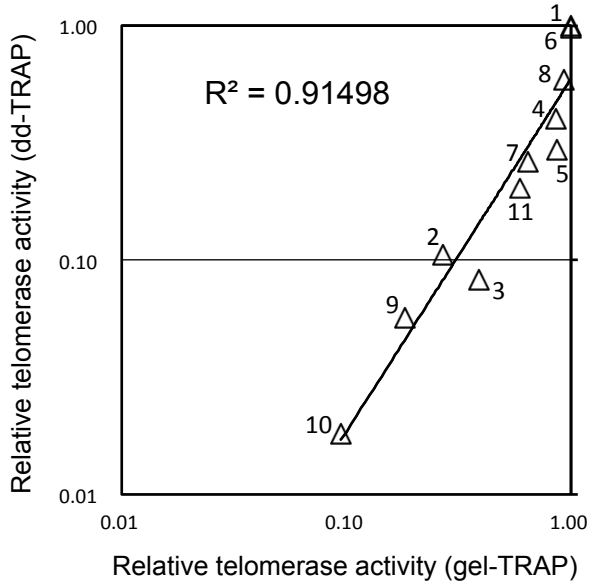

Figure 5

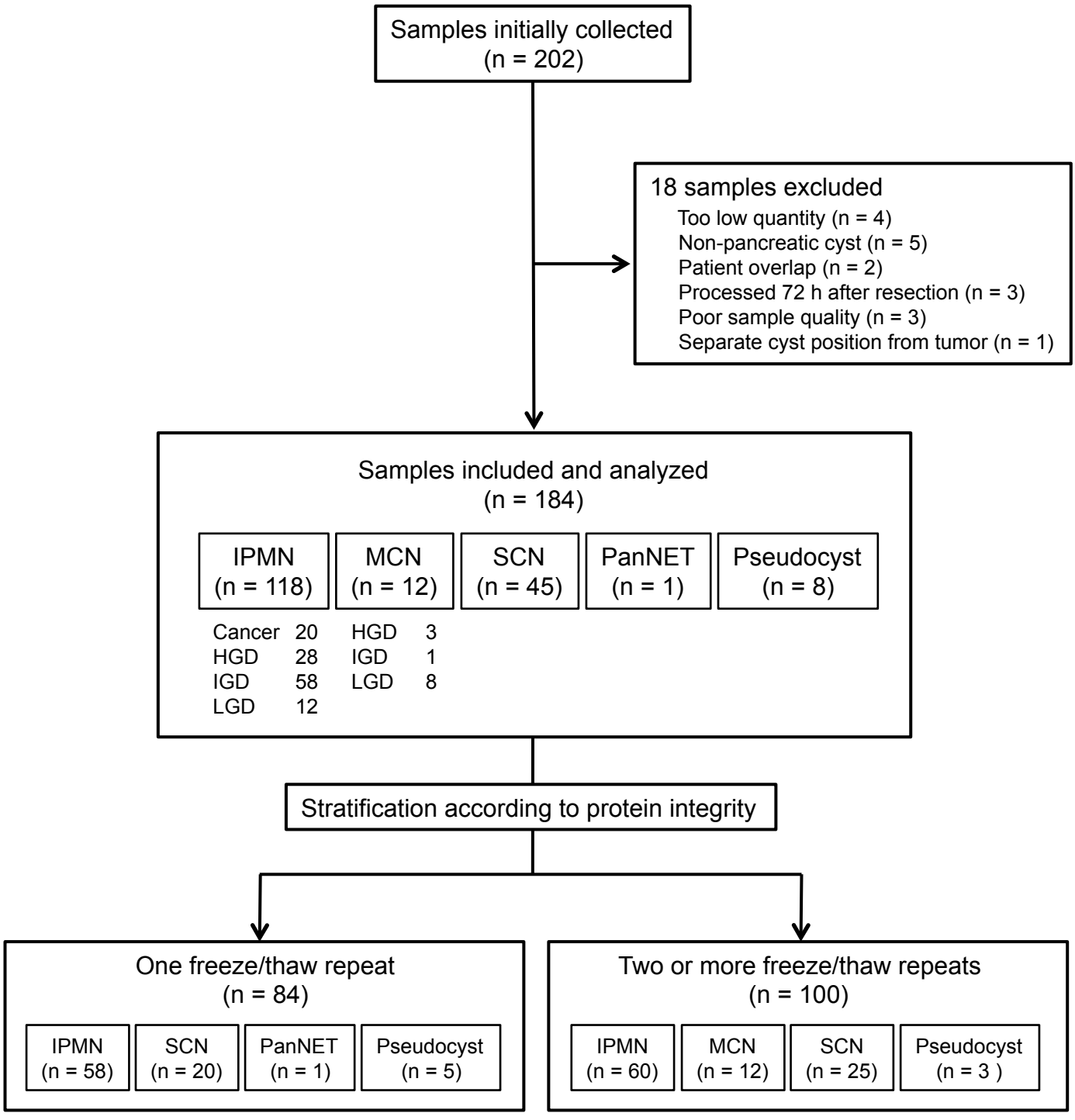
Samples initially collected
(n = 202)
18 samples excluded
Too low quantity (n = 4)
Non-pancreatic cyst (n = 5)
Patient overlap (n = 2)
Processed 72 h after resection (n = 3)
Poor sample quality (n = 3)
Separate cyst position from tumor (n = 1)
Samples included and analyzed
(n = 184)
IPMN
(n = 118)
MCN
(n = 12)
SCN
(n = 45)
PanNET
(n = 1)
Pseudocyst
(n = 8)
Cancer 20
HGD 28
IGD 58
LGD 12
HGD 3
IGD 1
LGD 8
Stratification according to protein integrity
One freeze/thaw repeat
(n = 84)
IPMN
(n = 58)
SCN
(n = 20)
PanNET
(n = 1)
Pseudocyst
(n = 5)
Two or more freeze/thaw repeats
(n = 100)
IPMN
(n = 60)
MCN
(n = 12)
SCN
(n = 25)
Pseudocyst
(n = 3)

Figure 6

A

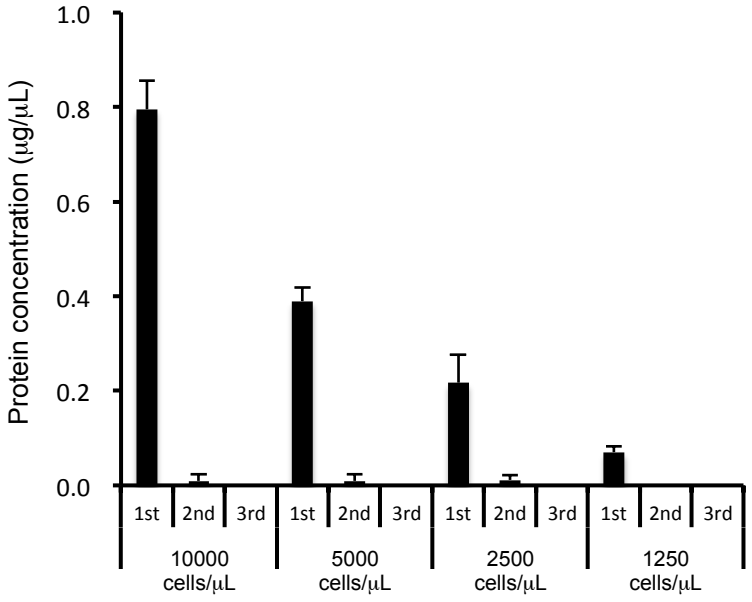
1.0
0.8
0.6
0.4
0.2
0.0
Protein concentration (μg/μL)
1st
2nd
3rd
10000 cells/μL
5000 cells/μL
2500 cells/μL
1250 cells/μL

B

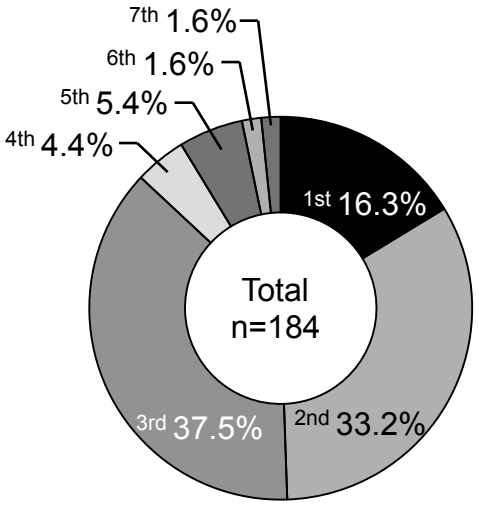
7th 1.6%
6th 1.6%
5th 5.4%
4th 4.4%
1st 16.3%
Total n=184
3rd 37.5%
2nd 33.2%

Figure 7

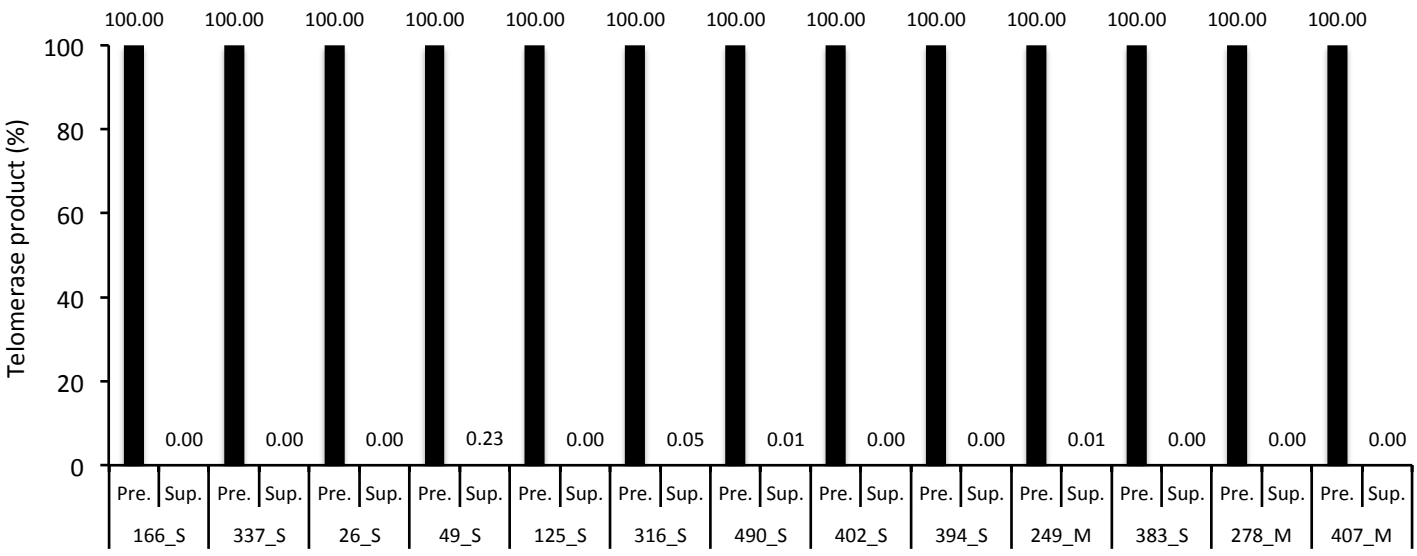
Telomerase product (%)
100
80
60
40
20
0
100.00
0.00
0.00
0.00
0.23
0.00
0.05
0.01
0.00
0.00
0.01
0.00
0.00
0.00
Pre.
Sup.
166_S
337_S
26_S
49_S
125_S
316_S
490_S
402_S
394_S
249_M
383_S
278_M
407_M

Figure 8

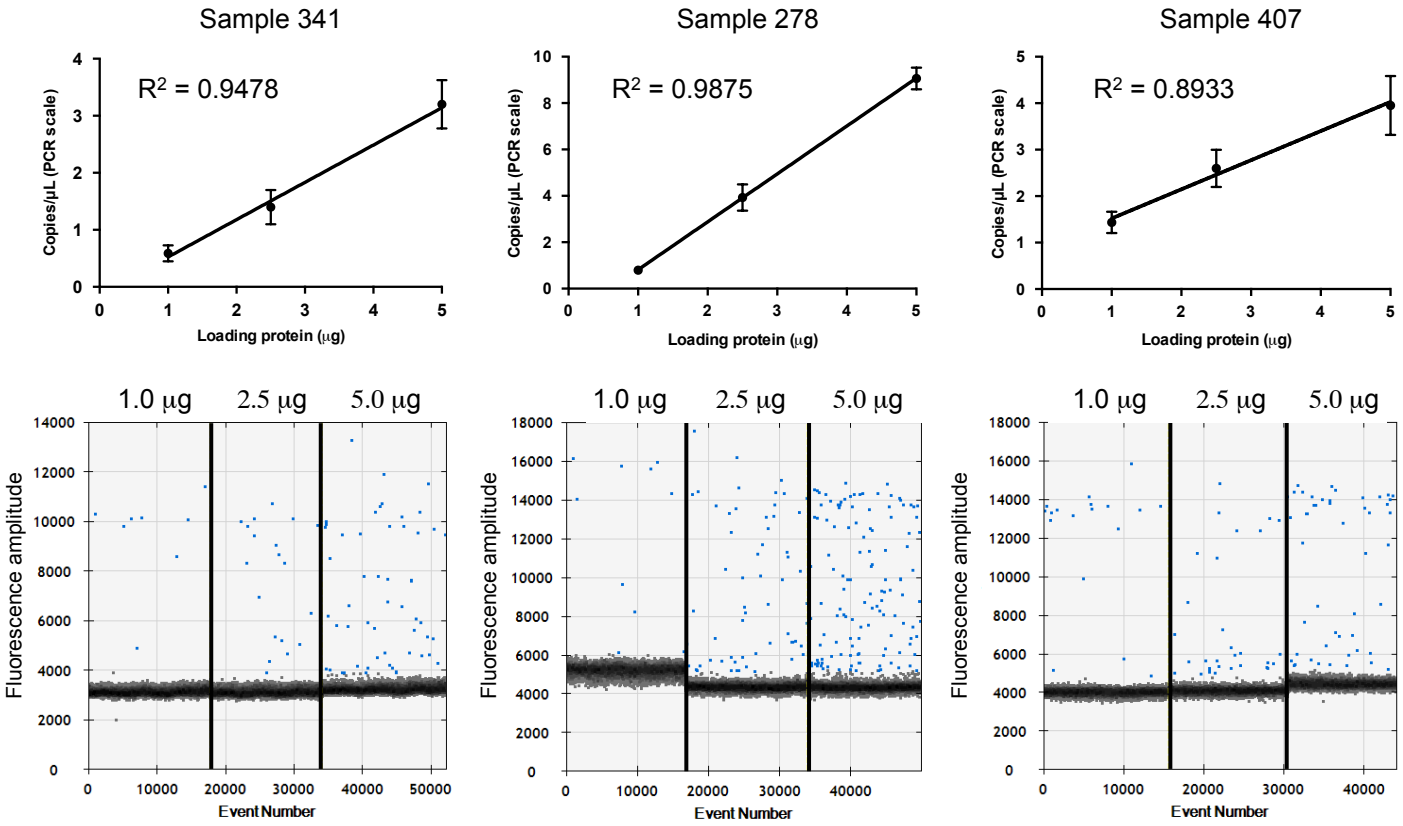
Sample 341
R² = 0.9478
Copies/µL (PCR scale)
Loading protein (µg)
Sample 278
R² = 0.9875
Copies/µL (PCR scale)
Loading protein (µg)
Sample 407
R² = 0.8933
Copies/µL (PCR scale)
Loading protein (µg)
1.0 µg
2.5 µg
5.0 µg
Fluorescence amplitude
Event Number
1.0 µg
2.5 µg
5.0 µg
Fluorescence amplitude
Event Number
1.0 µg
2.5 µg
5.0 µg
Fluorescence amplitude
Event Number

Figure 9

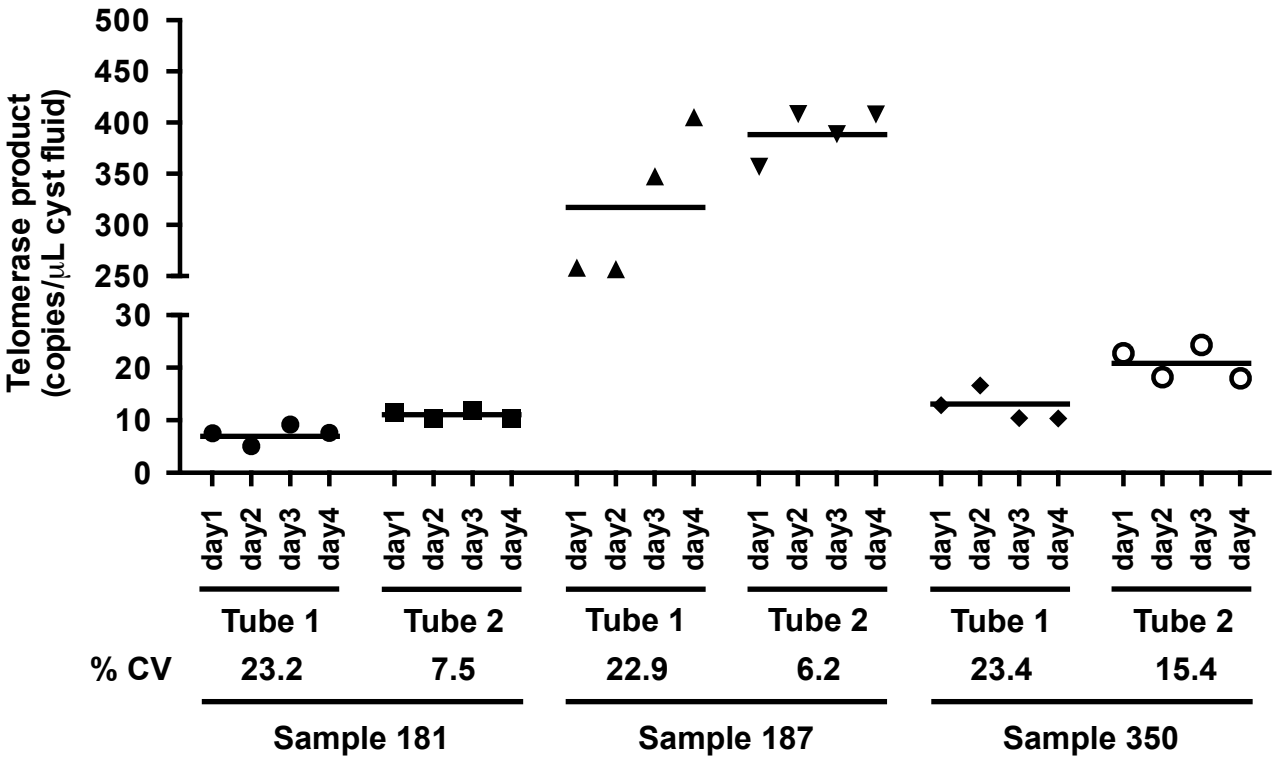
Telomerase product
(copies/μL cyst fluid)
500
450
400
350
300
250
30
20
10
0
day1
day2
day3
day4
Tube 1
Tube 2
% CV
23.2
7.5
22.9
6.2
23.4
15.4
Sample 181
Sample 187
Sample 350

Figure 10

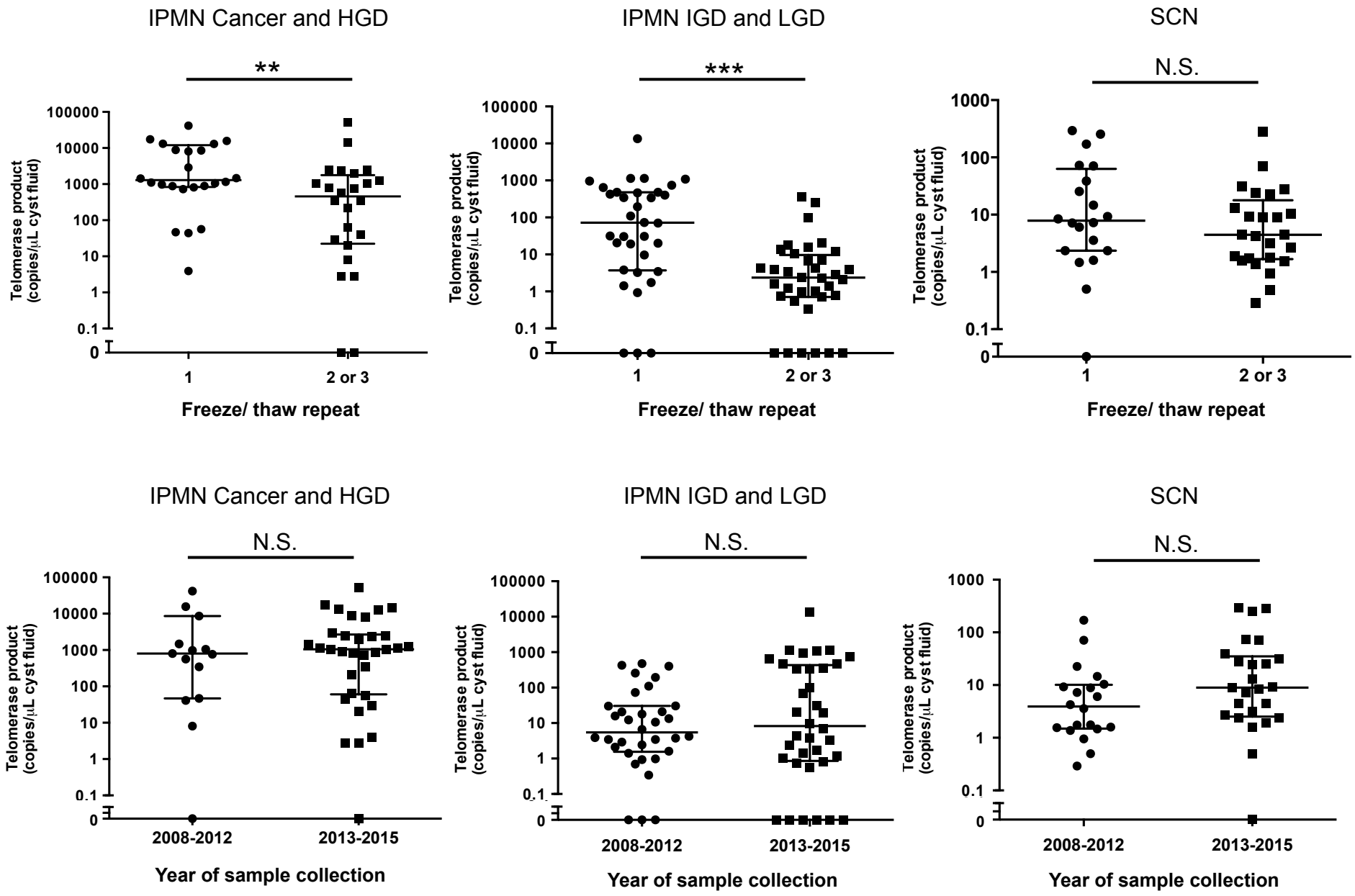
IPMN Cancer and HGD
**
Telomerase product (copies/μL cyst fluid)
100000
10000
1000
100
10
1
0.1
0
1
2 or 3
Freeze/ thaw repeat
IPMN IGD and LGD
***
Telomerase product (copies/μL cyst fluid)
100000
10000
1000
100
10
1
0.1
0
1
2 or 3
Freeze/ thaw repeat
SCN
N.S.
Telomerase product (copies/μL cyst fluid)
1000
100
10
1
0.1
0
1
2 or 3
Freeze/ thaw repeat
IPMN Cancer and HGD
N.S.
Telomerase product (copies/μL cyst fluid)
100000
10000
1000
100
10
1
0.1
0
2008-2012
2013-2015
Year of sample collection
IPMN IGD and LGD
N.S.
Telomerase product (copies/μL cyst fluid)
100000
10000
1000
100
10
1
0.1
0
2008-2012
2013-2015
Year of sample collection
SCN
N.S.
Telomerase product (copies/μL cyst fluid)
1000
100
10
1
0.1
0
2008-2012
2013-2015
Year of sample collection

Figure 11

A

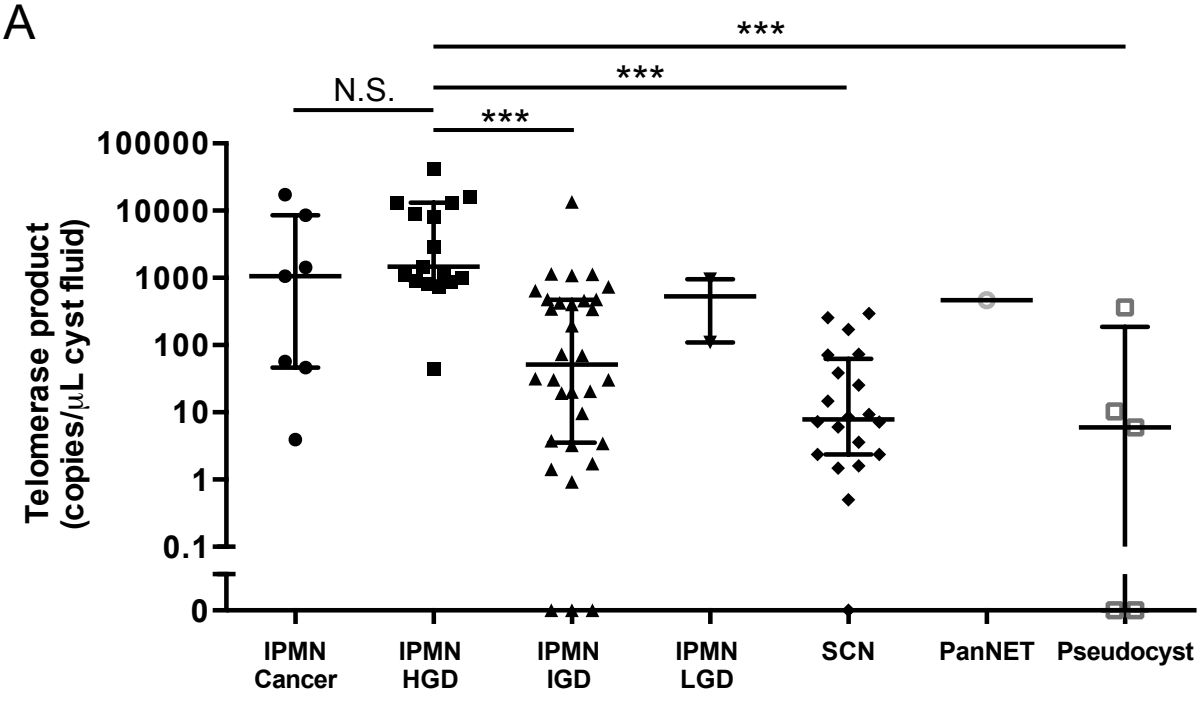

B

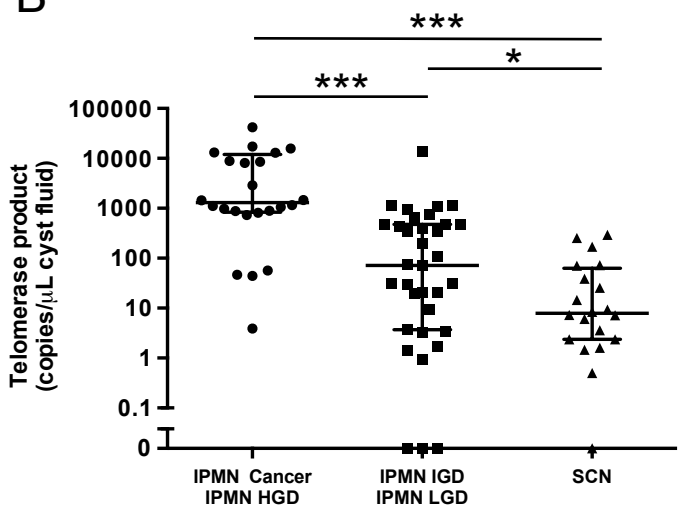

C

		n	Median	IQR
IPMN				
	Cancer	7	1055.0	(46.5–8576.0)
	HGD	17	1472.0	(884.9–13076.0)
	IGD	32	51.2	(3.5–473.4)
	LGD	2	533.8	(109.8–957.7)
SCN		20	7.9	(2.4–62.8)
PanNET		1	464.7	
Pseudocyst		5	6.0	(0.001–186.0)
IPMN cancer, HGD		24	1299.0	(830.2–11980.0)
IPMN IGD, LGD		34	72.0	(3.7–478.0)

D

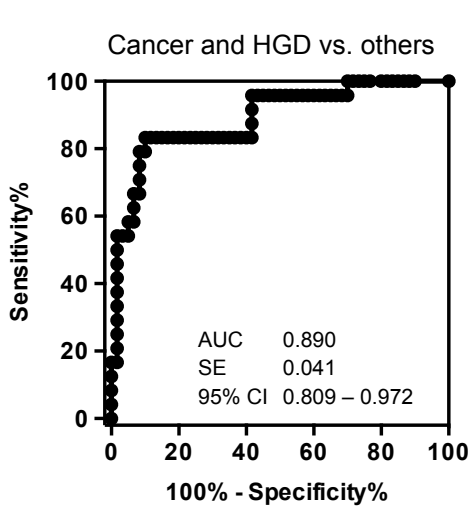

E

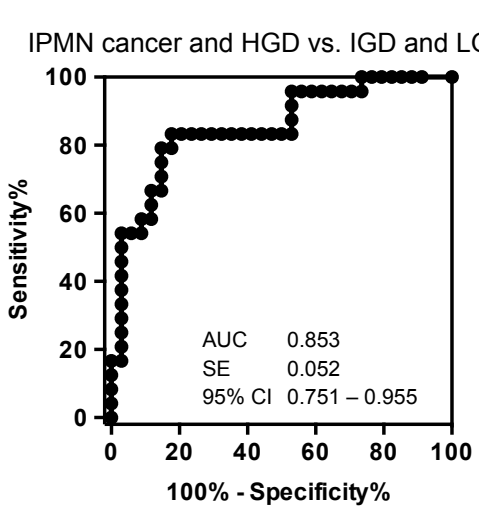

Figure 12

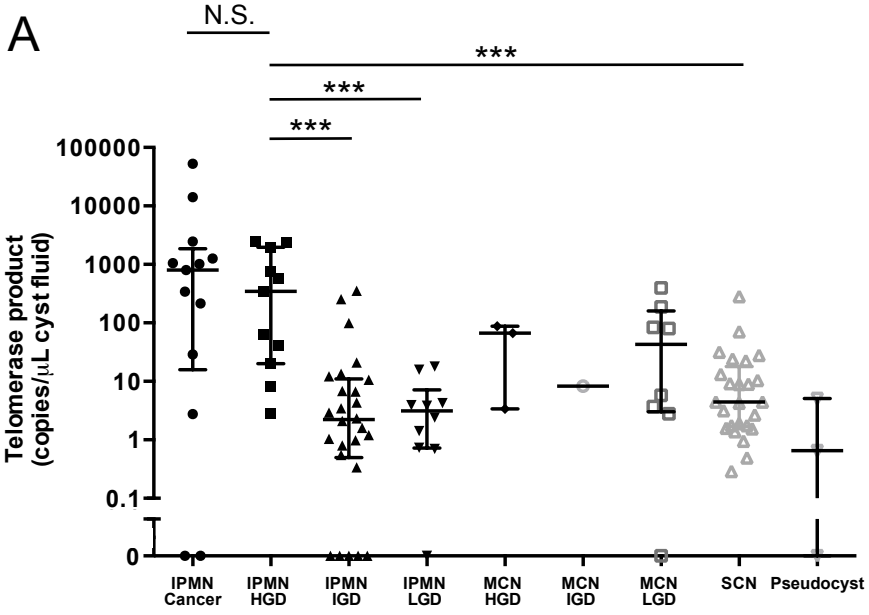
A
N.S.
***
***
***
Telomerase product (copies/μL cyst fluid)
100000
10000
1000
100
10
1
0.1
0
IPMN Cancer
IPMN HGD
IPMN IGD
IPMN LGD
MCN HGD
MCN IGD
MCN LGD
SCN
Pseudocyst

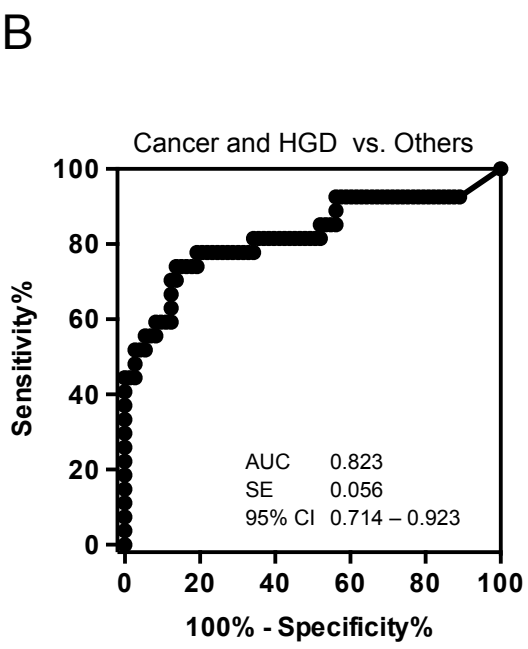
B
Cancer and HGD vs. Others
Sensitivity%
100% - Specificity%
AUC 0.823
SE 0.056
95% CI 0.714 – 0.923

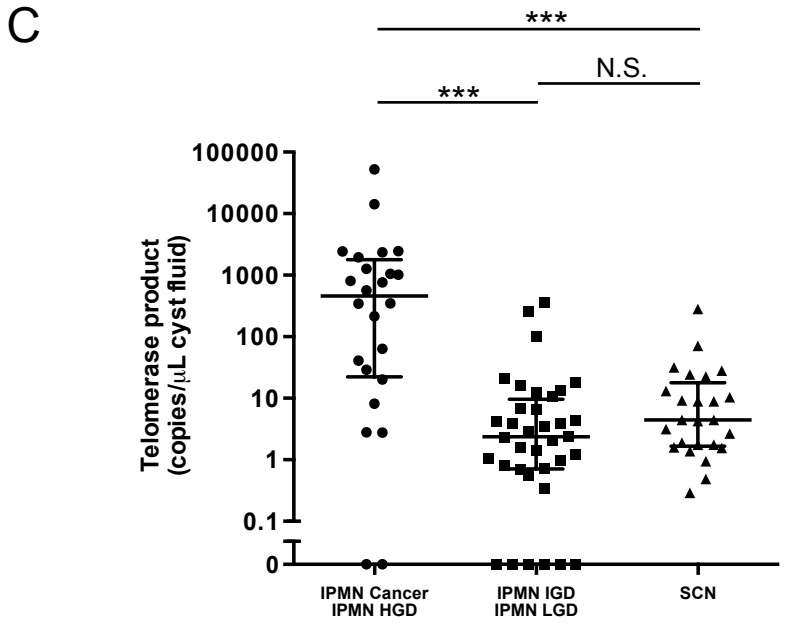
C
***
N.S.
***
Telomerase product (copies/μL cyst fluid)
100000
10000
1000
100
10
1
0.1
0
IPMN Cancer IPMN HGD
IPMN IGD IPMN LGD
SCN

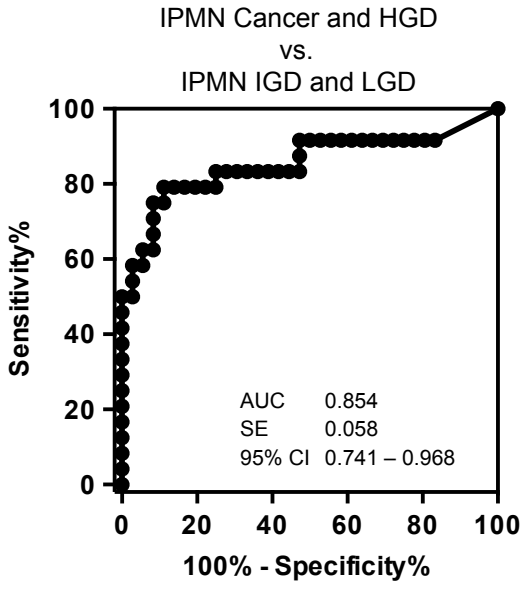
D
IPMN Cancer and HGD
vs.
IPMN IGD and LGD
Sensitivity%
100% - Specificity%
AUC 0.854
SE 0.058
95% CI 0.741 – 0.968

Figure 13

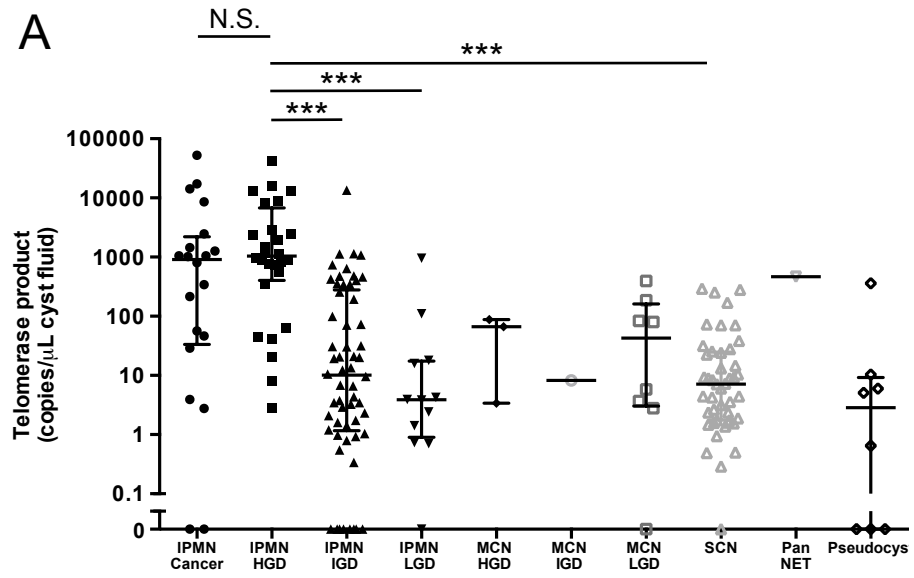
A
N.S.
***
***
***
Telomerase product (copies/μL cyst fluid)
100000
10000
1000
100
10
1
0.1
0
IPMN Cancer
IPMN HGD
IPMN IGD
IPMN LGD
MCN HGD
MCN IGD
MCN LGD
SCN
Pan NET
Pseudocys

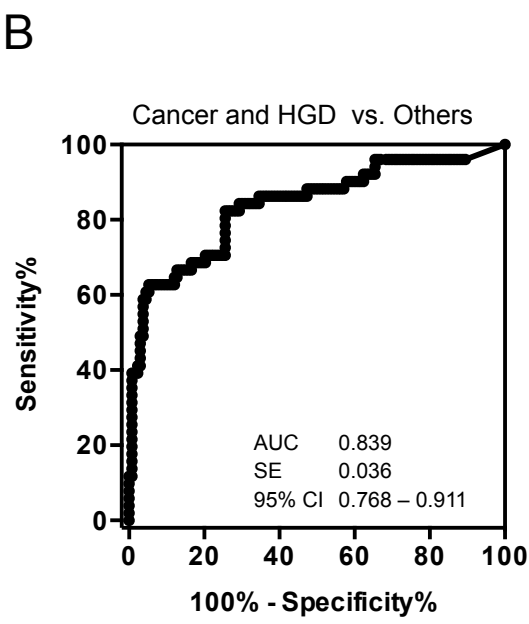
B
Cancer and HGD vs. Others
Sensitivity%
100
80
60
40
20
0
AUC 0.839
SE 0.036
95% CI 0.768 – 0.911
0
20
40
60
80
100
100% - Specificity%

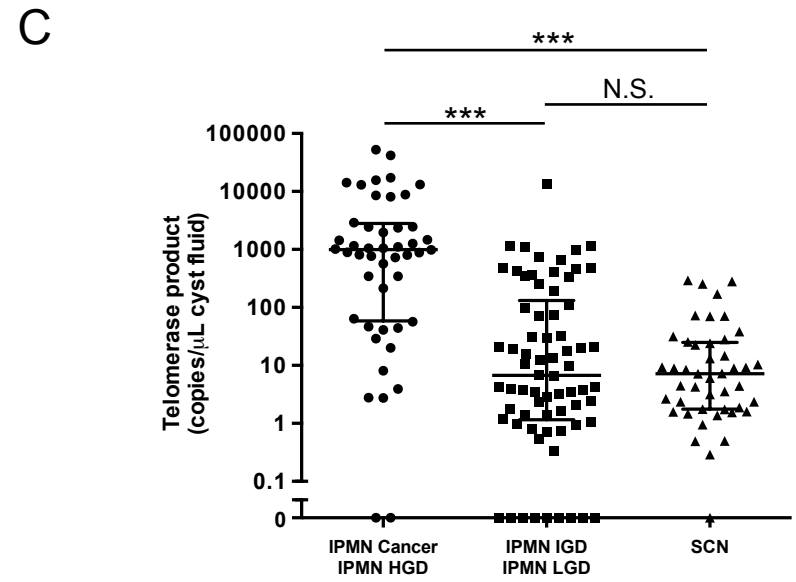
C
***
N.S.
***
Telomerase product (copies/μL cyst fluid)
100000
10000
1000
100
10
1
0.1
0
IPMN Cancer
IPMN HGD
IPMN IGD
IPMN LGD
SCN

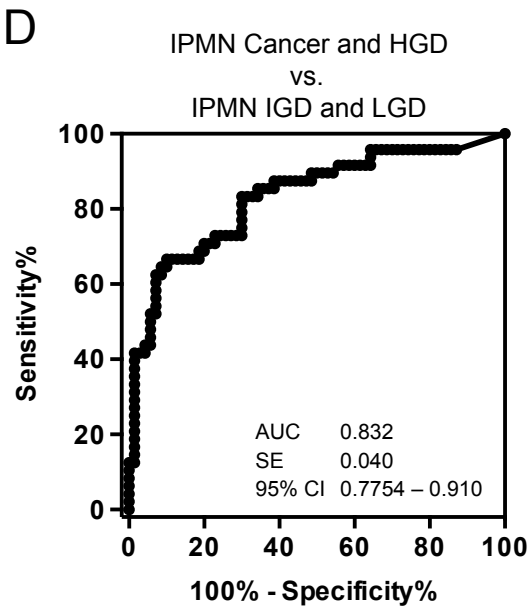
D
IPMN Cancer and HGD
vs.
IPMN IGD and LGD
Sensitivity%
100
80
60
40
20
0
AUC 0.832
SE 0.040
95% CI 0.7754 – 0.910
0
20
40
60
80
100
100% - Specificity%

Figure 14

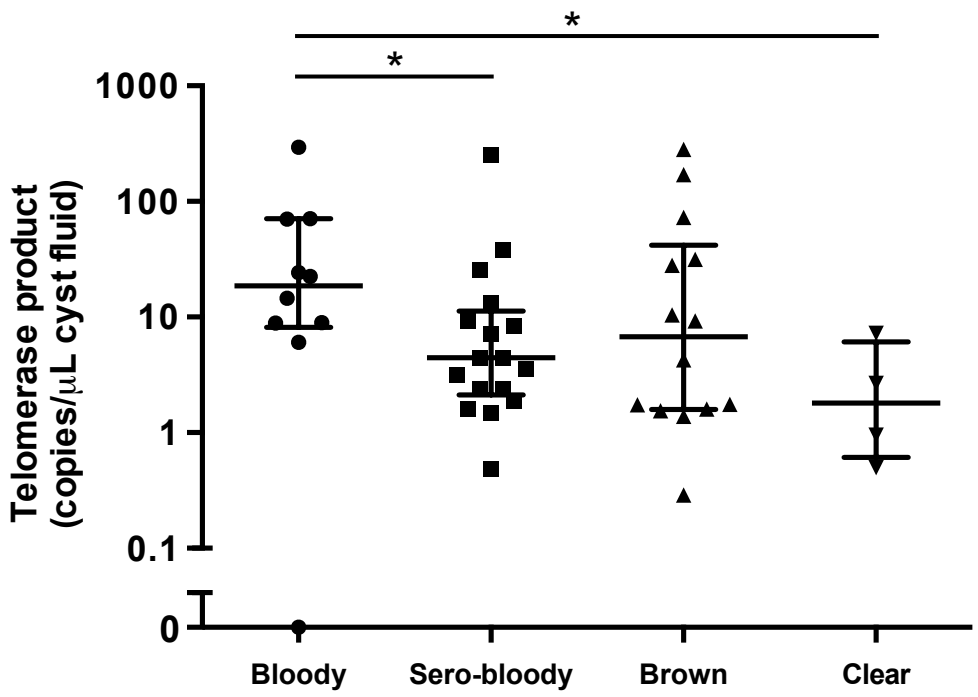
*
*
1000
100
10
1
0.1
0
Telomerase product
(copies/μL cyst fluid)
Bloody
Sero-bloody
Brown
Clear

Figure 15

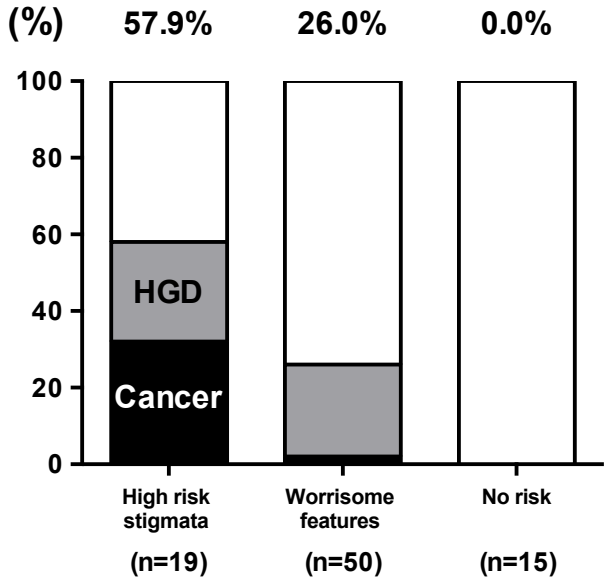
(%)
57.9%
26.0%
0.0%
100
80
60
40
20
0
HGD
Cancer
High risk stigmata
Worrisome features
No risk
(n=19)
(n=50)
(n=15)

Table 1. Clinical and imaging features of pancreatic cystic tumor for the aseeement of preoperative risk of malignancy.

High-risk stigmata	
	Obstructive jaundice with cystic lesion
	Enhancing solid component within cyst
	MPD size of ≥ 10 mm
Worrisome features	
	Cyst size of ≥ 30 mm
	Thickened/enhancing cyst walls
	MPD size of ≥ 5 mm
	Non-enhanced mural nodule
	Abrupt change in the MPD with distal pancreatic atrophy
	Pancreatitis
	Lymphadenopathy

Table 2. Patient and cyst fluid characteristics for all 184 cases.

Characteristics	Total (n = 184)	IPMN (n = 118)	MCN (n = 12)	SCN (n = 45)	PanNET (n = 1)	Pseudocyst (n = 8)
Male/Female (n)	83/101	65/53	0/12	13/32	0/1	5/3
Age (median, range), year	67 (27–87)	68 (42–87)	47 (28–65)	60 (30–85)	54	57 (27–82)
Symptoms						
Abdominal pain	42	21	7	12	0	2
Pancreatitis	10	10	0	0	0	0
Jaundice	4	4	0	0	0	0
Weight loss	1	1	0	0	0	0
Appetite loss	2	1	0	1	0	0
Nausea	2	1	0	1	0	0
Cyst location						
Head and uncinate/ body and tail	98/86	74/44	0/12	19/26	1/0	4/4
Cyst size, median (range), cm	3.0 (0.5–20.0)	2.5 (0.5–10.0)	4.7 (1.6–20.0)	4.0 (1.5–13.5)	5	3.4 (1.3–11.5)
Mural nodule						
Absent/Present	126/58	77/41	11/1	33/12	0/1	5/3
Communication with MPD						
Absent/Present	110/74	51/67	12/0	38/7	1/0	8/0
Dilatation of MPD ≥10mm						
Absent/Present	159/25	93/25	12/0	45/0	1/0	8/0
Dilatation of MPD ≥5mm						
Absent/Present	131/53	68/50	12/0	43/2	1/0	7/1
CT/MRI findings						
Worrisome features	118	61	11	37	1	8
High-risk stigmata	39	37	0	2	0	0
no risk	27	20	1	6	0	0

Table 2. Patient and cyst fluid characteristics for all 184 cases (Cont'd)

Characteristics	Total (n = 184)	IPMN (n = 118)	MCN (n = 12)	SCN (n = 45)	PanNET (n = 1)	Pseudocyst (n = 8)
Cyst fluid color						
Bloody/Sero-bloody/Brown/Straw/Clear	28/72/37/5/42	18/50/17/3/30	0/1/4/0/7	10/17/14/0/4	0/1/0/0/0	0/3/2/2/1
Cyst fluid appearance						
Serous/Mucinous	103/81	49/69	10/2	43/2	0/1	7/1
Original cyst volume (median, range), μL	250 (40–1000)	200 (40–1000)	350 (200–600)	400 (150–1000)	200	50 (50–1000)
EUS-FNA (n = 76)						
Non-diagnostic	15	7	2	6	0	0
Benign/Atypia/Cancer	32/16/13	18/15/13	5/1/0	7/0/0	0/0/0	2/0/0
Cyst fluid CEA (≥192 ng/mL), n = 44						
<192 ng/mL/≥192 ng/mL	30/14	13/11	4/3	12/0	0/0	1/0
Operative procedure						
PD/DP/TP/MP	97/81/5/1	73/40/4/1	0/12/0/0	19/26/0/0	0/0/1/0	5/3/0
Morphological duct type						
Main duct/Branch duct		29/89				
Grade of dysplasia						
LGD/IGD/HGD/Cancer	20/59/31/20	12/58/28/20	8/1/3/0		NET G2*	

IPMN, intraductal papillary mucinous neoplasm; MCN, mucinous cystic neoplasm; SCN, serous cystic neoplasm; PanNET, pancreatic neuroendocrine tumor; MPD, main pancreatic duct; CT, computed tomography; MRI, magnetic resonance imaging; EUS-FNA, endoscopic ultrasonography-fine needle aspiration, CEA, carcinoembryonic antigen; PD, pancreaticoduodenectomy; DP, distal pancreatectomy; TP, total pancreatectomy. MP, middle pancreatectomy; HGD, high grade dysplasia; IGD, intermediate grade dysplasia; LGD, low grade dysplasia.

*Histological grade of PanNET was diagnosed on the basis of WHO 2010 criteria.

Table 3. Length of storage and freeze and thaw repeats of surgically aspirated pancreatic cyst fluid samples.

Findings	Total (n = 184)
Year of sample collection	
2008	3
2009	1
2010	17
2011	31
2012	27
2013	31
2014	42
2015	32
Freeze and thaw repeat(s)	
1	84
2	93
3	7

Table 4. Patient and cyst fluid characteristics for 84 cases without prior thaw/freezing.

Characteristics	Total (n = 84)	IPMN (n = 58)	SCN (n = 20)	PanNET (n = 1)	Pseudocyst (n = 5)
Male/Female (n)	45/39	35/23	6/14	0/1	4/1
Age (median, range), year	68 (37–87)	68 (42–87)	64 (37–77)	54	73 (54–82)
Symptoms					
Abdominal pain	16	10	4	0	2
Pancreatitis	7	7	0	0	0
Jaundice	1	1	0	0	0
Nausea	1	0	1	0	0
Cyst location					
Head and uncinate/ body and tail	46/38	33/25	10/10	1/0	2/3
Cyst size, median (range), cm	2.5 (0.5–11.5)	2.3 (0.5–9.0)	3.2 (1.5–10.0)	5	3.8 (2.5–11.5)
Mural nodule					
Absent/Present	50/34	33/25	13/7	0/1	4/1
Communication with MPD					
Absent/Present	43/41	22/36	15/5	1/0	5/0
Dilatation of MPD ≥10mm					
Absent/Present	71/13	45/13	20/0	1/0	5/0
Dilatation of MPD ≥5mm					
Absent/Present	56/28	32/26	19/1	1/0	4/1
CT/MRI findings					
Worrisome features	50	31	13	1	5
High-risk stigmata	19	17	2	0	0
no risk	15	10	5	0	0
Cyst fluid color					
Bloody/Sero-bloody/Brown/Straw/Clear	19/36/9/5/15	14/24/4/3/13	5/10/3/0/2	0/1/0/0/0	0/1/2/2/0

Table 4. Patient and cyst fluid characteristics for 84 cases without prior thaw/freezing (Cont'd)

Characteristics	Total (n = 84)	IPMN (n = 58)	SCN (n = 20)	PanNET (n = 1)	Pseudocyst (n = 5)
Cyst fluid appearance					
Serous/Mucinous	39/45	17/41	18/2	0/1	4/1
Original cyst volume (median, range), μL	150 (40–1000)	103 (40–800)	300 (150–1000)	200	50 (50–200)
EUS-FNA (n = 30)					
Non-diagnostic	4	1	3	0	0
Benign/Atypia/Cancer	11/8/7	8/8/7	3/0/0	0/0/0	0/0/0
Cyst fluid CEA (≥192 ng/mL), n = 17					
<192 ng/mL/≥192 ng/mL	12/5	6/5	6/0	0/0	0/0
Operative procedure					
PD/DP/TP/MP	47/34/2/1	34/22/1/1	11/9/0/0	0/0/1/0	2/3/0/0
Morphological duct type					
Main duct/Branch duct		14/44			
Grade of dysplasia					
LGD/IGD/HGD/Cancer		2/32/17/7		NET G2	

IPMN, intraductal papillary mucinous neoplasm; SCN, serous cystic neoplasm; PanNET, pancreatic neuroendocrine tumor; MPD, main pancreatic duct; CT, computed tomography; MRI, magnetic resonance imaging; EUS-FNA, endoscopic ultrasonography-fine needle aspiration, CEA, carcinoembryonic antigen; PD, pancreaticoduodenectomy; DP, distal pancreatectomy; TP, total pancreatectomy. MP, middle pancreatectomy; HGD, high grade dysplasia; IGD, intermediate grade dysplasia; LGD, low grade dysplasia.

*Histological grade of PanNET was diagnosed on the basis of WHO 2010 criteria.

Table 5. Diagnostic performance of telomerase activity comparing to the multiple imaging and clinical factors.

Findings	Cut-off	Sensitivity (%) (95% CI)	Specificity (%) (95% CI)	Accuracy (%)	PPV (%)	NPV (%)
All cases (n = 84)						
Cyst appearance	Mucinous	87.5 (67.6–97.3)	60.0 (46.5–72.4)	67.9	46.7	92.3
Cyst size	≥30 mm	41.7 (22.2–63.4)	61.7 (48.2–73.9)	56.0	30.3	72.6
MPD dilatation	≥10 mm	33.3 (15.6–55.3)	91.7 (81.6–97.2)	75.0	61.5	77.5
MPD dilatation	≥5 mm	66.7 (44.7–84.4)	80.0 (67.7–89.2)	76.2	57.1	85.7
Mural nodule	Present	62.5 (40.6–81.2)	68.3 (55.0–79.7)	66.7	44.1	82.0
Telomerase activity	≥730 copies/μL cyst fluid	83.3 (62.6–95.3)	90.0 (79.5–96.2)	88.1	76.9	93.1
IPMN cases (n = 58)						
Cyst appearance	Mucinous	87.5 (67.6–97.3)	41.2 (24.6–59.3)	60.3	51.2	82.4
Cyst size	≥30 mm	41.7 (22.2–63.4)	70.6 (52.5–84.9)	58.6	50.0	63.2
MPD dilatation	≥10 mm	33.3 (15.6–55.3)	85.3 (68.9–95.1)	63.8	61.5	64.4
MPD dilatation	≥5 mm	66.7 (44.7–84.4)	70.6 (52.5–84.9)	69.0	61.5	75.0
Mural nodule	Present	62.5 (40.6–81.2)	70.6 (52.5–84.9)	67.2	60.0	72.7
Telomerase activity	≥730 copies/μL cyst fluid	83.3 (62.6–95.3)	82.4 (65.5–93.2)	82.8	76.9	87.5

MPD, main pancreatic duct; CI, confidence interval; PPV, positive predictive value; NPV, negative predictive value

Table 6. Diagnostic performance of combination assay for predicting invasive cancer or high-grade dysplasia among 84 cases without prior freeze/thawing.

Any of these present			Sensitivity (%)	Specificity (%)	Accuracy (%)
Imaging findings		Telomerase activity (copies/μL cyst fluid)			
Any of these present	MPD ≥10 mm	None	33.3	91.7	75.0
		≥730	87.5	83.3	84.5
		≥814	87.5	85.0	85.7
	Mural nodule	None	62.5	68.3	66.7
		≥730	95.8	66.7	75.0
	MPD ≥10 mm Mural nodule	None	70.8	63.3	65.5
		≥730	100.0	61.7	72.6
All of these present	MPD ≥10 mm Mural nodule	None	25.0	96.7	76.2
		≥730	50.0	90.0	78.6

MPD, main pancreatic duct

Table 7. Univariate and multivariate analyses of malignant predictive factors for pancreatic cystic tumor.

Variable	Cancer, HGD (n = 24)	Others (n = 60)	Univariate	Multivariate		
			P	OR	95% CI	*P*
Age						
<68	11	30	0.7300			
≥68	13	30				
Sex						
Female	8	31	0.1280			
Male	16	29				
Fluid appearance						
Serous	3	36	**<0.0001**	1.000		
Mucinous	21	24		0.727	0.034–6.405	0.787
Cyst size						
<30 mm	14	37	0.7775			
≥30 mm	10	23				
Cyst location						
Body and tail	8	30	0.1656			
Head	16	30				
MPD dilatation						
<5 mm	8	48	**<0.0001**	1.000		
≥5 mm	16	12		0.931	0.137–5.059	0.936
MPD communication						
Absent	5	38	**0.0004**	1.000		
Present	19	22		3.242	0.630–18.057	0.157
Mural nodule						
Absent	9	41	**0.0093**	1.000		
Present	15	19		1.278	0.273–5.364	0.743
Telomerase activity						
<730 copies/μL (cyst fluid)	4	54	**<0.0001**	1.000		
≥730 copies/μL (cyst fluid)	20	6		41.488	4.897–992.730	**0.0002**

HGD, high grade dysplasia; OR, odds ratio; CI, confidence interval; MPD, main pancreatic duct.

Table 8. Diagnostic performance of telomerase activity in stratified subgroup by the risk of malignancy.

Subgroup	n	AUC	Cut off*	TP	FN	FP	TN	Sensitivity (%) (95% CI)	Specificity (%) (95% CI)	Accuracy (%)	PPV (%)	NPV (%)
All cases (n = 84)												
High-risk stigmata	19	0.784	730	8	3	1	7	72.7 (39.0–94.0)	87.5 (47.4–99.7)	78.9	88.9	70.0
Worrisome features	50	0.927	730	12	1	5	32	92.3 (64.0–99.8)	86.5 (71.2–95.5)	88.0	70.6	97.0
IPMN cases (n = 58)												
High-risk stigmata	17	0.758	730	8	3	1	5	72.7 (39.0–94.0)	83.3 (35.9–99.6)	76.5	88.9	62.5
Worrisome features	31	0.876	730	12	1	5	13	92.3 (64.0–99.8)	72.2 (46.5–90.3)	83.9	70.6	92.9

***** Value of telomerase activity in pancreatic cyst fluid (copies/μL of cyst fluid).

AUC, area under the curve; TP, true positive; FN, false negative; FP, false positive; TN, true negative; PPV, positive predictive value; NPV, negative predictive value.

Table 9. List of matched cases with endoscopically and surgically aspirated cyst fluid samples.

Case No.	Age	Sex	Tumor location	Endoscopically aspirated cyst fluid				From EUS to Ope. (month)	Operative Procedures	Surgically aspirated cyst fluid	
				CEA (ng/mL)	Amylase (U/L)	Telomerase activity*	Histocytological diagnosis			Telomerase activity*	Histological diagnosis
1	54	F	Tail	61.6	99	0.00	Non-diagnostic	8.9	DP	0.00	Pseudocyst
2	73	F	Body	<1.0	31	2.41	Non-diagnostic	14.3	DP	2.36	SCN
3	78	M	Head	168.0	N/A	20.29	Benign	9.3	PD	13118.29	IPMN with HGD

*Copies/μL of original cyst fluid

EUS, Endoscopic ultrasonography; DP, diatal pancreatectomy; PD, pancreaticoduodenectomy